

NBER WORKING PAPER SERIES

THE ECONOMIC GEOGRAPHY OF GLOBAL WARMING

Jose Luis Cruz Alvarez  
Esteban Rossi-Hansberg

Working Paper 28466  
<http://www.nber.org/papers/w28466>

NATIONAL BUREAU OF ECONOMIC RESEARCH  
1050 Massachusetts Avenue  
Cambridge, MA 02138  
February 2021

We thank Klaus Desmet, Per Krusell and participants at numerous seminars and conferences for their feedback. We also thank the International Economics Section at Princeton University for financial support. The views expressed herein are those of the authors and do not necessarily reflect the views of the National Bureau of Economic Research.

NBER working papers are circulated for discussion and comment purposes. They have not been peer-reviewed or been subject to the review by the NBER Board of Directors that accompanies official NBER publications.

© 2021 by Jose Luis Cruz Alvarez and Esteban Rossi-Hansberg. All rights reserved. Short sections of text, not to exceed two paragraphs, may be quoted without explicit permission provided that full credit, including © notice, is given to the source.

The Economic Geography of Global Warming  
Jose Luis Cruz Alvarez and Esteban Rossi-Hansberg  
NBER Working Paper No. 28466  
February 2021  
JEL No. F63,F64,Q51,Q54,Q56

### **ABSTRACT**

Global warming is a worldwide and protracted phenomenon with heterogeneous local economic effects. In order to evaluate the aggregate and local economic consequences of higher temperatures, we propose a dynamic economic assessment model of the world economy with high spatial resolution. Our model features a number of mechanisms through which individuals can adapt to global warming, including costly trade and migration, and local technological innovations and natality rates. We quantify the model at a  $1^\circ \times 1^\circ$  resolution and estimate damage functions that determine the impact of temperature changes on a region's fundamental productivity and amenities depending on local temperatures. Our baseline results show welfare losses as large as 15% in parts of Africa and Latin America but also high heterogeneity across locations, with northern regions in Siberia, Canada, and Alaska experiencing gains. Our results indicate large uncertainty about average welfare effects and point to migration and, to a lesser extent, innovation as important adaptation mechanisms. We use the model to assess the impact of carbon taxes, abatement technologies, and clean energy subsidies. Carbon taxes delay consumption of fossil fuels and help flatten the temperature curve but are much more effective when an abatement technology is forthcoming.

Jose Luis Cruz Alvarez  
Department of Economics  
Princeton University  
Princeton, NJ 08544  
jlca@princeton.edu

Esteban Rossi-Hansberg  
Princeton University  
Department of Economics  
289 Julis Romo Rabinowitz Building  
Princeton, NJ 08544-1021  
and CEPR  
and also NBER  
erossi@princeton.edu

An online appendix is available at <http://www.nber.org/data-appendix/w28466>

# 1 Introduction

The world is getting warmer due to carbon emissions generated by the economic activity of humans. Global carbon emissions will affect temperatures everywhere over long periods of time and in geographically heterogeneous ways. What will be the impact of carbon emissions, and the implied changes in temperatures, on the world economy and on the economy of particular regions? How will individuals react to these changes and how are these reactions impacted by their ability to migrate, trade, or invest and develop alternative centers of economic activity? What are the best policies to combat global warming and what are their implications for different regions across the world? In this paper we propose and quantify a novel global spatial dynamic assessment model to address these questions.

The nature of the global warming phenomenon determines the elements of our assessment model. Global carbon emissions affect local temperatures around the world, so we want a model of the world economy. Because these effects are extremely heterogeneous across regions, even within countries, we want a model with local geographic detail where temperatures affect both productivity and the living amenities from residing in particular locations. Agents facing adverse temperature conditions that affect their welfare in a given location will react by moving, by trading with other locations, and by developing centers of economic activity in areas that are not so heavily affected or that benefit from warmer temperatures. Hence, we require a model with costly trade and migration, as well as private technological investments. We also need to introduce clean and carbon-based energy as inputs in production so that fossil fuels create carbon dioxide emissions, which in turn affect global and local temperatures through a global carbon cycle and a temperature down-scaling model. Because global warming is a protracted phenomenon developing over hundreds of years and happening in a growing economy, we need an assessment model that is dynamic and incorporates the implications of this growth on carbon emissions and adaptation over time. Such a model will also allow us to study and understand the dynamic implications of this phenomenon across locations. Once we incorporate dynamics over long periods of time, we also need to incorporate population changes by means of birth and mortality rates that vary across regions with different incomes and temperatures.

Our starting point is the spatial growth framework in [Desmet et al. \(2018\)](#). We model trade, migration, and innovation as in that paper. We add clean and carbon-based energy as inputs in production with imperfect substitutability, a carbon extraction technology that determines its cost as a function of the stock of carbon extracted, and the associated carbon cycle that determines global temperature and, through a local down-scaling factor, local temperatures. We model the effect of local temperature on fundamental productivities and amenities through two distinct damage functions that determine the impact of temperature changes on each local characteristic, as a function of the current temperature. The estimated functions indicate, as expected, that warm regions' productivities and amenities are impacted negatively by increases in temperatures, while the opposite is the case for the coldest regions. We also incorporate fertility into the model, so every period agents living at a particular location have a natality rate (birth minus death rate)

that depends on their income and the local temperature. This adds local and global population dynamics to our model.

We quantify the model devoting particular attention to identify the effect that changes in local climatic conditions have on local productivities and amenities. We start by using data from G-Econ, the Human Development Index, together with a number of parameters obtained from the literature, to invert the model and obtain the local productivities and amenities that rationalize populations and income every five year-period from 1990 to 2005 (the years for which G-Econ is available). This model inversion also yields the migration costs that rationalize population movements across regions given the natality function we estimate using United Nations net natality rates. We then use the fundamental productivities and amenities to estimate how they are affected by changes in local temperatures. Because these fundamental productivities and amenities come from a model with costly trade, migration, innovation, and fertility, these adaptation mechanism are already taken explicitly into account. This is clearly preferable to estimating damage functions from endogenous outcomes like output or population. We estimate the effect of climate on these fundamentals allowing for the semi-elasticity to depend on local temperatures and include location as well as time fixed effects. The estimated damage functions yield significant effects of changes in temperature for wide ranges of initial current temperatures, but they also yield relatively large confidence intervals that we use to assess the uncertainty underlying our results.

The final step in the quantification is to parameterize the effect of carbon use for future carbon extraction costs and the carbon cycle. We model energy as a constant elasticity of substitution composite between fossil fuels and clean energy. The cost of these two sources of energy evolves with the world's endogenous technology, but the cost of fossil fuels also depends on the amount of carbon that has been used in the past, since the remaining stock is increasingly harder to extract. Using data from [Bauer et al. \(2017\)](#), we estimate a convex relationship between cumulative emissions and the cost of extraction. Firms decide on their use of fossil fuels, which leads to carbon emissions. A standard carbon cycle model (as in [IPCC \(2013\)](#)) then generates global temperature dynamics.<sup>1</sup> Our baseline analysis matches the global temperature dynamics from 2000 to 2400 in the IPCC RCP 8.5 scenario almost exactly. To down-scale from global to local temperatures we follow [Mitchell \(2003\)](#) and use a linear function with heterogeneous local factors that we estimate as a function of a large number of local characteristics.<sup>2</sup> The estimated down-scaling factors (the local temperature change for a one degree change in global temperature) can be as large as 2.5 in parts of Siberia and Alaska and as low as 0.5 in parts of Asia and South America.

With the quantified model in hand, we can simulate the economy forward over several centuries and evaluate the economic consequences of global warming. This phenomenon is expected to have heterogeneous effects over space, where the hottest regions in South America, Africa, India and Australia experience

---

<sup>1</sup>We also include exogenous CO<sub>2</sub> emissions from forestry and non-CO<sub>2</sub> greenhouse gasses from RCP 8.5.

<sup>2</sup>We use Chebyshev polynomials of order 10 in latitude, longitude, elevation, distance to coast, distance to ocean, distance to water, vegetation density and albedo.

welfare losses of 15% and the coldest regions in Alaska, Northern Canada, and Siberia undergo welfare gains as high as 14%. On average, the world is expected to lose 6% in terms of welfare, although the exact number depends on the yearly discount factor.<sup>3</sup> By 2200, the average loss in welfare is 10% and in output larger than 4%, although the uncertainty inherited from our estimated damage functions implies that the 95% confidence intervals include losses as high as 20% and 12%, respectively. The large uncertainty in average outcomes, however, does not translate into significant uncertainty on the spatial distribution of losses. The relative distribution of losses is very similar in our baseline case compared to the worst or the best-case scenarios (as measured by the 95% confidence intervals of our damage functions). When we decompose the losses coming from the effect of global warming on amenities or productivity we find that about half of the average effects come from the impact of temperature rise on productivity. Effects on amenities are particularly important for losses in Africa and gains at the most northern latitudes; while losses in productivity affect almost all regions to the south of the 30° latitude.

Our evaluation of the effects of global warming emphasizes economic adaptation through migration, trade, and endogenous local innovation. We assess the importance of each of these adaptation channels using counterfactuals that increase the cost of migrating, trading, or investing by a certain percent globally. If we increase migration costs by 25% throughout the globe, the average cost of global warming rises by an additional 4% by the year 2200. Higher migration costs make global warming more costly for Africa, but also for northern regions that benefit less from the influx of migrants. Increases in migration costs lead to significantly faster population growth as more people stay in poorer areas where they have more children. Compared to migration, we find a substantially smaller impact from increases in trade costs. The reason is that the evolution of temperature is spatially correlated, and most trade is local. Furthermore, our model features trade, but only an aggregate sector and therefore no adaptation through sectoral specialization.<sup>4</sup> Innovation is somewhere in between, a rise in innovation costs has a large relative effect that benefits the coldest places but hurts the warmest ones significantly. On average, though, less innovation implies that regions in India and China, that will eventually be heavily affected by global warming, grow less and so the world on average loses less from the rise in temperatures.

The last part of the paper uses our quantified model to evaluate a number of environmental policies. The equilibrium allocation in the modeled economy is not efficient due to carbon emissions being a global externality, but also due to the presence of production externalities, technology diffusion, and congestion externalities. We study taxes on carbon dioxide, subsidies on clean energy, and the importance of abatement technologies that eliminate the pernicious effects of carbon. Clean energy subsidies have only a modest effect on carbon emissions and the corresponding evolution of global temperature since, although they generate substitution towards clean energy, they also lead to a reduction in the price of energy which results

---

<sup>3</sup>In our baseline scenario we use a discount factor of  $\beta = 0.965$  in an economy where real GDP grows around 3% per year.

<sup>4</sup>See [Conte et al. \(2020\)](#) for a related model that incorporates an agricultural and a non-agricultural sector and where trade plays a more important role as an adaptation mechanism.

in more production and ultimately more energy use. These effects tend to cancel each other out.

Carbon taxes have a larger effect on CO<sub>2</sub> emissions and temperatures. The reduction in the use of fossil fuels leads to less carbon emissions which results in lower temperatures that persist for hundreds of years. However, the reduction in carbon use also implies that more carbon is left unexploited on Earth, which yields lower future extraction costs. The implication is that carbon taxes primarily delay the use of the carbon on Earth, rather than decreasing its total use. This has the effect of *flattening* the temperature curve, with lower temperatures for long periods of time, but with little impact over the very long-run. Hence, the effects of carbon taxes on the environment are primarily concentrated in the next 100 years or so. Of course, this result also implies that carbon taxes can be particularly effective in combination with abatement technologies. If abatement technologies are forthcoming, delaying carbon consumption has tremendously positive effects since the effect of future emissions is abated using the new technology. Thus, our results strongly suggest that carbon taxes should be combined with incentives to invent effective abatement technologies. To use an analogy from the epidemiology literature, flattening an infection curve is particularly effective if a cure is forthcoming, but much less so otherwise.<sup>5</sup>

Standard models of global warming use aggregate loss functions that relate the future path of the aggregate economy to the evolution of climate variables. In many cases, these loss functions fail to incorporate the behavioral responses of individuals and firms. Because those functions are not derived from micro-founded models in which optimal behavior is obtained as a response to climatic shocks, they fail to consider that households and firms can adapt, although bearing costs, to the most salient consequences of this phenomenon. Incorporating these responses is particularly important because of the vast heterogeneity that rising temperatures will have on the fundamentals of the economy. It is also essential, because only a model that explicitly takes into account these behavioural adaptation responses across regions can properly account for potential changes in aggregate loss functions in policy counterfactuals and simulations of alternative scenarios (an expression of the Lucas critique, [Lucas \(1976\)](#)). A quantitative dynamic model like ours, with individual behavioural responses and an explicit treatment of spatial heterogeneity at a high resolution is, therefore, a needed addition to the economics of climate change.

In the last decade there has been a surge of empirical estimates of climate damages that use panel methodologies and exploit short-run weather variation to identify the causal effect of temperature on economic and social outcomes. This wave of empirical papers was pioneered by the work of [Deschênes and Greenstone \(2007\)](#), who study the impact of temperature on agricultural profits. This methodology has been employed to quantify the weather effects on mortality ([Barreca et al. \(2016\)](#), [Carleton et al. \(2020\)](#)),

---

<sup>5</sup>As we know from standard Pigovian analysis we can address the negative externality created by fossil fuels using taxes that increase their price. However, another potentially effective strategy is to increase the elasticity of substitution between fossil fuels and clean sources in the technology to produce energy. In the aggregate, this elasticity is not a fundamental parameter of technology, but rather a parameter that aggregates the many ways the world has to produce energy. As such, this parameter is not necessarily either constant or policy invariant. Although we use estimates in the literature and fix it at 1.6 in our baseline scenario, we show that increases in this elasticity can be extremely effective in reducing the use of fossil fuels over time as extraction costs rise. Such an increase in this elasticity can be achieved, for example, by switching vehicles to use energy from all sources, as electric cars do.

amenities (Albouy et al. (2016), Baylis (2020)), crime and conflict (Burke et al. (2015a)), migration (Missirian and Schlenker (2017)), crop yields (Schlenker and Roberts (2009)), GDP and GDP growth (Dell et al. (2012), Burke et al. (2015b)).<sup>6</sup> This work has been useful to provide evidence of the link between temperature and economic outcomes, but it cannot be used to determine the future effects of temperature across regions, or to evaluate different policies.

Some of these estimates have been incorporated in economic models of global warming, also known as Integrated Assessment Models (IAM), to quantify the economic consequences of this phenomenon. The most popular models tend to consider coarse geographical units and display a limited role for adaptation mechanisms in mediating climate damages (Nordhaus (2017), Anthoff and Tol (2014), Hope and Hope (2013), IPCC (2013), Golosov et al. (2014)). A notable exception is Krusell and Smith (2017), who consider a spatial resolution similar to ours but, in contrast to us, consider the effect of global warming on local capital investments. We depart from their work, by explicitly incorporating trade, migration, innovation, and population growth, and by estimating the damage functions on productivities and amenities, rather than GDP.

These core models have been extended to analyze different dimensions of global warming. Popp (2004), Acemoglu et al. (2012), Acemoglu et al. (2016), Acemoglu et al. (2019), Hassler et al. (2019) assess the role of clean technology investments and innovations in mitigating climate damages. Benveniste et al. (2020) explore the extent to which migration and border policies attenuate the level of exposure and vulnerability to climate change impacts. Dietz and Lanz (2020) study the capacity to meet food demand for different climate change conditions. Fried (2019) evaluates the role of investment in adaptation capital to reduce damages from extreme weather. Hassler et al. (2018) compare the warming-induced losses in GDP and the optimal carbon taxes, when considering extreme values for the climate sensitivity and economic damages. Costinot et al. (2016) examine the losses in the agriculture sector when trade and production patterns are allowed to adjust across different crops. Barrage (2019) studies the optimal environmental policy in the presence of distortionary taxes.

We contribute to the development of IAMs by incorporating recent developments in spatial quantitative models. In particular, we build on Desmet et al. (2018), that develops a spatial growth theory at a fine level of geographical resolution and analyzes the evolution of the economy over several centuries. The static spatial component resembles Allen and Arkolakis (2014), but adds costly migration, and the dynamic component follows Desmet and Rossi-Hansberg (2014).<sup>7</sup> We incorporate local fertility and population dynamics, energy use, fossil fuels extraction costs, a carbon cycle, effects of temperature on productivity and amenity, among other features to these existing economic frameworks.

There is an incipient literature that addresses environmental questions through the lens of spatial dynamic models. Balboni (2019) quantifies the cost of road investment in the coasts of Vietnam under the

---

<sup>6</sup>Dell et al. (2014) and Auffhammer (2018) review this body of research.

<sup>7</sup>See Redding and Rossi-Hansberg (2017) for a survey of this literature.

presence of sea level rise. [Desmet et al. \(2021\)](#) measure the spatial shifts in population and economic activity due to sea level rise, using a highly spatially disaggregated model, closer to ours. [Desmet and Rossi-Hansberg \(2015\)](#), [Nath \(2020\)](#) and [Conte et al. \(2020\)](#) evaluate the impact of global warming across different economic sectors which is something we do not incorporate in this paper. Relative to them, we add realistic spatial heterogeneity, dynamics and high spatial resolution, and population dynamics and effects of temperature on amenities, respectively. Ultimately, our aim is to generate a model with all the necessary elements to serve as a workhorse for a new generation of IAMs models that incorporate dynamics, rich spatial heterogeneity, and micro-founded adaptation mechanisms.

The rest of the paper is structured as follows. Section 2 presents the economic and climate model. Section 3 quantifies the model and estimates the damage functions. Section 4 describes the baseline quantitative implications of global warming. Section 5 discusses the role of the different forms of adaptation in mediating the harmful effects of global warming. Section 6 analyzes the effect of a number of environmental policies. Section 7 concludes.

## 2 The Model

The economic component of the model extends [Desmet et al. \(2018\)](#) among a number of dimensions. First, we incorporate an endogenous law of motion for global population. Second, we consider that production requires labor, land, and energy. Energy comes from fossil fuels or clean sources. The former type of energy generates CO<sub>2</sub> emissions, whereas the latter does not. Third, local climate conditions distort the fundamental amenities, productivities, and natality rates in spatially heterogeneous ways.

The carbon cycle and the global temperature modules are based on the reduced-form models in [IPCC \(2013\)](#). The projection from global to local temperature follows the statistical down-scaling approach, formalized by [Mitchell \(2003\)](#).

### 2.1 Endowment and Preferences

The world economy occupies a two-dimensional surface  $S$ , where a location is defined as a point  $r \in S$  with land density  $H(r)$ . In each period  $t$ ,  $L_t$  agents live in the world economy. Global population is time-dependent due to endogenous natality rates.

Every period, agents derive utility from consuming a set of differentiated varieties  $c_t^\omega(r)$  aggregated according to a CES utility function, from local amenities,  $b_t(r)$ , and from their idiosyncratic preference for the location where they live,  $\varepsilon_t^i(r)$ . If agents move from  $r$  to  $s$  at  $t$ , utility is discounted by mobility costs,  $m(r, s)$ , which are paid as a permanent flow cost from  $t$  onward. Specifically, the period utility of agent  $i$



who resides in  $r$  in period  $t$  and has a location history  $r_- = (r_0, \dots, r_{t-1})$  is given by

$$u_t^i(r_-, r) = \left[ \int_0^1 c_t^\omega(r)^\rho d\omega \right]^{1/\rho} b_t(r) \varepsilon_t^i(r) \prod_{s=1}^t m(r_{s-1}, r_s)^{-1}. \quad (1)$$

Agents earn income from work. They inelastically supply one unit of labor and receive a wage  $w_t(r)$ . They also receive a share of land rents,  $H(r)R_t(r)$ , which are uniformly distributed across a location's residents. Thus, per capita real income is  $y_t(r) = (w_t(r) + R_t(r)/L_t(r))/P_t(r)$ , where  $L_t(r)$  denotes local population density (population per unit of land) and  $P_t(r)$  the local ideal CES price index.

Local amenities  $b_t(r)$  are affected by congestion according to  $b_t(r) = \bar{b}_t(r)L_t(r)^{-\lambda}$ , where  $\bar{b}_t(r)$  represents a location's *fundamental* amenities and  $\lambda$  the congestion elasticity of amenities to population density. Fundamental amenities can be distorted by local climate conditions through the *damage* function  $\Lambda^b(\cdot)$ . This function denotes the percentage change in fundamental amenities when local temperature rises from  $T_{t-1}(r)$  in period  $t-1$  to  $T_t(r) = \Delta T_t(r) + T_{t-1}(r)$  in period  $t$ . Namely,

$$\bar{b}_t(r) = (1 + \Lambda^b(\Delta T_t(r), T_{t-1}(r))) \bar{b}_{t-1}(r) \quad (2)$$

Hence, when  $\Lambda^b(\Delta T_t(r), T_{t-1}(r))$  is negative (positive), amenities in cell  $r$  are damaged (improved) by increases in local temperature. The dependence of the damage function on the level of temperature, and not only on the change in temperature, captures the heterogeneous impacts over space that global warming is expected to have. Naturally, and as we estimate in Section 3, the amenities in hot places (like Congo) decline with further increases in temperature, whereas amenities in cold places (like Siberia) benefit from warmer climate.

Households also experience idiosyncratic taste shocks,  $\varepsilon_t^i(r)$ , that we assume are independent and identically distributed across households, locations, and time according to a Fréchet distribution with shape parameter  $1/\Omega$  and scale parameter 1. A greater value of  $\Omega$  implies more dispersion in agent's tastes across locations, acting as a second congestion force.

We assume that the flow-utility cost of moving from  $r$  to  $s$  is given by the product of an origin-specific cost,  $m_1(r)$ , and a destination-specific cost,  $m_2(s)$ , so  $m(r, s) = m_1(r)m_2(s)$ . Note that, since staying in the same location is costless,  $m(r, r) = 1$ , origin costs are simply the inverse of destination costs, namely  $m_1(r) = 1/m_2(r)$ . Hence, the permanent utility cost of entering a location is compensated by a permanent utility benefit when leaving, which implies that agents only pay the flow cost while residing there. This way of modelling migration costs implies that migration decisions are reversible and, therefore, the location choice of agents only depends on current variables and not on past or future ones. As is standard in discrete choice models with idiosyncratic preferences, the fraction of households residing in  $r$  at period  $t$  is then

given by

$$\frac{L_t(r)H(r)}{L_t} = \frac{u_t(r)^{1/\Omega} m_2(r)^{-1/\Omega}}{\int_S u_t(v)^{1/\Omega} m_2(v)^{-1/\Omega} dv}, \quad (3)$$

where  $u_t(r)$  denotes the component of local utility that is not idiosyncratic, namely,

$$u_t(r) = b_t(r)y_t(r) = b_t(r) \left[ \int_0^1 c_t^\omega(r)^\rho d\omega \right]^{1/\rho}. \quad (4)$$

At the end of period  $t$ , after the migration decisions have been made, each household has  $n_t(r)$  net off-springs. Local natality rates are exogenous to the individual but endogenous to a location's real income and local temperature,  $n_t(r) = \eta(y_t(r), T_t(r))$ . Therefore, at the beginning of period  $t + 1$ , before migration decisions are made, local population density  $L'_{t+1}(r)$  is determined by

$$L'_{t+1}(r)H(r) = (1 + n_t(r)) L_t(r)H(r). \quad (5)$$

Note that global population depends not only on the distribution of natality rates across space and time, and through them on the distribution of income and local temperatures, but also on the spatial distribution of population in the previous period.

## 2.2 Technology

In each cell there is a continuum of firms, producing differentiated varieties  $\omega \in [0, 1]$ . Output is produced using a constant returns to scale technology in land, labor, and energy. Output per unit of land of variety  $\omega$  is given by

$$q_t^\omega(r) = \phi_t^\omega(r)^{\gamma_1} z_t^\omega(r) (L_t^\omega(r)^\chi e_t^\omega(r)^{1-\chi})^\mu, \quad (6)$$

where  $L_t^\omega(r)$  and  $e_t^\omega(r)$  denote the production workers and the energy use, both per unit of land. Note that, since land is a fixed factor with share  $1 - \mu$ , agglomerating labor and energy in a location yields decreasing returns, which acts as a third congestion force.

A firm's productivity is determined by its innovation decision,  $\phi_t^\omega(r) \geq 1$ , and an idiosyncratic location-variety productivity shifter,  $z_t^\omega(r)$ . Firms can invest in innovation by paying a cost  $\nu \phi_t^\omega(r)^\xi$ , expressed in units of labor per land. The exogenous productivity shifter is the realization of a random variable which is independent and identically distributed across varieties and time according to a Fréchet distribution with cumulative distribution function  $F(z, a) = e^{-a_t(r)z^{-\theta}}$ . The scale parameter  $a_t(r)$  governs the level of productivity in a location and is affected by agglomeration externalities as a consequence of high population density and endogenous past innovations. In particular, we let  $a_t(r) = \bar{a}_t(r)L_t(r)^\alpha$  where  $\alpha$  governs the strength of the first agglomeration force.

The fundamental productivity,  $\bar{a}_t(r)$ , is in turn determined by an endogenous dynamic process given

by

$$\bar{a}_t(r) = (1 + \Lambda^a(\Delta T_t(r), T_{t-1}(r))) \left( \phi_{t-1}(r)^{\theta_{\gamma_1}} \left[ \int_S D(v, r) \bar{a}_{t-1}(v) dv \right]^{1-\gamma_2} \bar{a}_{t-1}(r)^{\gamma_2} \right). \quad (7)$$

Equation (7) has four components. The term  $\phi_{t-1}(r)^{\theta_{\gamma_1}}$  represents the shift in the local distribution of shocks that results from the last period's innovation decisions of firms, which are assumed to now be embedded in the local technology.<sup>8</sup> The individual contemporaneous effect of innovation affects the production function in (6) directly. The term  $\left[ \int_S D(v, r) \bar{a}_{t-1}(v) dv \right]^{1-\gamma_2} \bar{a}_{t-1}(r)^{\gamma_2}$  denotes the level of past technology that firms build on. It is composed of the location's own technology level  $\bar{a}_{t-1}(r)$ , as well as technology diffusion from other locations, where the function  $D(v, r)$  denotes the spatial decay in the strength of technology diffusion. This specification follows Desmet et al. (2018) closely and all its dynamic implications are developed and discussed there. It generates a spatial endogenous growth model. Important for our purposes is that we add the term  $\Lambda^a(\cdot)$ , which incorporates the effect of temperature on local productivity. When the damage function  $\Lambda^a(\Delta T_t(r), T_{t-1}(r))$  is negative (positive), productivity in cell  $r$  at time  $t$  declines (increases) due to temperature change. Since  $\Lambda^a(\cdot)$  depends on temperature levels, it is flexible to capture the heterogeneous spatial impacts of global warming on productivity.

Unlike Desmet et al. (2018), production does not only require land and labor, but also energy. Following Golosov et al. (2014), Hassler et al. (2019), and Popp (2006), among others, energy and other factors are aggregated through a Cobb Douglas production function where  $(1 - \chi)\mu$  denotes the share of energy in the production process. In turn, energy is a CES composite between fossil fuels,  $e_t^{f,\omega}(r)$ , and clean sources,  $e_t^{c,\omega}(r)$ , where the elasticity of substitution is given by  $\epsilon$ .<sup>9</sup> The use of fossil fuels generates CO<sub>2</sub> emissions, which accumulate in the atmosphere intensifying the greenhouse gas effect, whereas the use of clean energy does not. Specifically, we let

$$e_t^\omega(r) = \left( \kappa e_t^{f,\omega}(r)^{\frac{\epsilon-1}{\epsilon}} + (1 - \kappa) e_t^{c,\omega}(r)^{\frac{\epsilon-1}{\epsilon}} \right)^{\frac{\epsilon}{\epsilon-1}}, \quad (8)$$

where  $\kappa$  governs the relative productivity of both technologies in producing energy.

We assume competitive local energy markets and so the price of each type of energy is equal to its marginal production cost. Producing one unit of energy of type  $j \in \{f, c\}$  requires  $\mathcal{Q}_t^j(r)$  units of labor. The cost of energy varies across locations, time, and source, according to

$$\mathcal{Q}_t^f(r) = \frac{f(\text{CumCO2}_{t-1})}{\zeta_t^f(r)} \quad \text{and} \quad \mathcal{Q}_t^c(r) = \frac{1}{\zeta_t^c(r)}. \quad (9)$$

<sup>8</sup>As Desmet et al. (2018) shows, all firms in a given location and point in time make identical innovation decisions.

<sup>9</sup>This elasticity governs the extent to which energy sources might not be perfect substitutes due to their ease of use, their location, or the existence of technologies and capital designed to primarily use a particular source. We introduce it as a fixed parameter, but perform a number of counterfactual exercises to assess its impact.

The evolution of the cost of fossil fuel,  $Q_t^f(r)$ , is composed of two terms. The numerator denotes the cost of extracting fossil fuels from the ground, which we assume is increasing and convex in total world cumulative CO<sub>2</sub> emissions,  $CumCO2_{t-1}$ , following Nordhaus and Boyer (2002). As cumulative emissions increase, carbon reserves shrink, which rises the cost of extraction. Cumulative emissions are simply the sum of cumulative emissions in the previous period plus the global CO<sub>2</sub> emissions released at  $t$ ,  $E_t^f$ , namely

$$CumCO2_t = CumCO2_{t-1} + E_t^f = CumCO2_{t-1} + \int_S \int_0^1 e_t^{f,\omega}(v) H(v) d\omega dv. \quad (10)$$

The denominator of the energy price relates to the productivity,  $\zeta_t^j(r)$ , in energy generation of type  $j$ . We assume that the rate at which technology evolves over time in the fossil fuel and clean sector is related to global real GDP,  $y_t^w$ , which is endogenous in this model, as it depends on the investment decisions of firms. In particular, we consider that an increase of one percent in global real GDP rises log-productivity in energy generation by  $v^j$ , where this elasticity is allowed to vary across types of energy. That is,

$$\zeta_t^j(r) = \left( \frac{y_t^w}{y_{t-1}^w} \right)^{v^j} \zeta_{t-1}^j(r), \quad \text{where} \quad y_t^w = \int_S \left( \frac{L_t(v) H(v)}{L_t} \right) y_t(v) dv. \quad (11)$$

Consequently, firm's innovations generate an externality on energy productivity improvements with magnitude that depends on the evolution of real GDP.<sup>10</sup>

We also assume that land markets are competitive. Firms bid for land and the firm whose bid is the largest wins the right to produce in that parcel. This is important since past innovations, embedded in the level of the local idiosyncratic distribution of productivities, benefit all potential entrants. As proven in Desmet and Rossi-Hansberg (2014), this implies that the solution to the dynamic innovation problem of firms is to simply choose the level of innovation that maximizes their current profits (or equivalently their bid for land), since all future gains of current innovations will accrue to land, which is the fixed factor. Future firms profits are zero independently of a firm's actions and so do not affect its decisions. Since there is a continuum of potential entrants, firms end up bidding all of their profits after covering innovation costs. Hence, in this economy, firm profits are zero and the maximum bid for land is the local land price,  $R_t(r)$ , every period. In sum, firms in  $r$  simply maximize

$$\max_{q,L,\phi,e^f,e^c} p_t^\omega(r,r) q_t^\omega(r) - w_t(r) L_t^\omega(r) - w_t(r) \nu \phi_t^\omega(r)^\xi - w_t(r) Q_t^f(r) e_t^{f,\omega}(r) - w_t(r) Q_t^c(r) e_t^{c,\omega}(r) - R_t(r)$$

where  $q_t^\omega(r)$  is given by (6) and (8), and  $p_t^\omega(r,r)$  is the price at location  $r$  of variety  $\omega$  produced at  $r$ .

The first order conditions with respect to fossil fuel and clean energy allow us to rewrite the total energy cost in labor units as the energy composite  $e_t^\omega(r)$  times its ideal price index  $Q_t(r)$ . Namely,  $Q_t(r) e_t^\omega(r) =$

<sup>10</sup>An alternative approach would be to explicitly model the purposeful innovation decisions by firms that extract and distribute fossil fuels and generate clean energy, as we did for the technology of firms producing final goods. The aforementioned assumption simplifies the model and captures the reality of the many technological spillovers between industries.

$Q_t^f(r)e_t^{f,\omega}(r) + Q_t^c(r)e_t^{c,\omega}(r)$ , where

$$Q_t(r) = \left( \kappa^\epsilon Q_t^f(r)^{1-\epsilon} + (1-\kappa)^\epsilon Q_t^c(r)^{1-\epsilon} \right)^{\frac{1}{1-\epsilon}}. \quad (12)$$

Since technology is Cobb-Douglas, a firm's energy costs are proportional to labor costs, so  $Q_t(r)e_t^\omega(r) = \frac{1-\chi}{\chi} L_t^\omega(r)$ . Thus, the problem of the firm collapses to a problem parallel to the one posed by [Desmet et al. \(2018\)](#), and so all their results apply.

### 2.3 Prices, Export Shares, and Trade Balance

Goods markets are competitive, so firms sell goods at marginal cost after accounting for transport costs. Let  $\varsigma(s, r) \geq 1$  denote the iceberg trade cost of transporting a good from  $r$  to  $s$ . Then,

$$p_t^\omega(s, r) = \frac{\varsigma(s, r)mc_t(r)}{z_t^\omega(r)}, \quad (13)$$

where  $mc_t(r)$  denotes the marginal input cost at location  $r$ , which is common across firms since they face the same prices and therefore make the same decisions. The marginal input costs is given by

$$mc_t(r) = \mathcal{M}Q_t(r)^{(1-\chi)\mu}w_t(r)^{\mu+\gamma_1/\xi}R_t(r)^{1-\mu-\gamma_1/\xi}, \quad (14)$$

where  $\mathcal{M}$  is a proportionality constant that depends on production parameters.

As is standard in trade structures based on [Eaton and Kortum \(2002\)](#), the probability,  $\pi_t(s, r)$ , that a good produced in  $r$  is consumed at  $s$  is then given by a gravity equation of the form

$$\pi_t(s, r) = \frac{a_t(r)[mc_t(r)\varsigma(r, s)]^{-\theta}}{\int_S a_t(v)[mc_t(v)\varsigma(v, s)]^{-\theta} dv}. \quad (15)$$

and the price index,  $P_t(r)$ , of a location (where  $\Gamma(\cdot)$  denotes the Gamma function) by

$$P_t(r) = \Gamma\left(\frac{-\rho}{(1-\rho)\theta+1}\right)^{-\frac{1-\rho}{\rho}} \left[ \int_S a_t(v)[mc_t(v)\varsigma(r, v)]^{-\theta} dv \right]^{-1/\theta}. \quad (16)$$

Finally, since we are interested in outcomes over long periods of time, we impose trade balance cell by cell, so that total income (labor income plus land rents) at  $r$  equals the total expenditure on goods from  $r$ . Namely,

$$w_t(r)L_t(r)H(r) = \int_S \pi_t(v, r)w_t(v)L_t(v)H(v)dv. \quad (17)$$

## 2.4 Climate and the Carbon Cycle

The burning of fossil fuels (as well as other activities, like deforestation) leads to emissions of carbon dioxide into the atmosphere. The carbon cycle defines how carbon flows accumulate in the atmosphere. The evolution of atmospheric CO<sub>2</sub> follows the dynamics proposed by [IPCC \(2013\)](#) where the stock of carbon in the atmosphere,  $S_t$ , evolves according to

$$S_{t+1} = S_{\text{pre-ind}} + \sum_{\ell=1}^{\infty} (1 - \delta_{\ell}) \left( E_{t+1-\ell}^f + E_{t+1-\ell}^x \right). \quad (18)$$

As defined in (10),  $E_t^f$  denotes the endogenous CO<sub>2</sub> emissions from fossil fuel combustion. In addition,  $E_t^x$  are exogenous CO<sub>2</sub> emissions from non-fuel combustion, taken from the Representative Consumer Pathway (RCP) 8.5 IPCC scenario. The parameter  $S_{\text{pre-ind}}$  denotes the CO<sub>2</sub> stock in the pre-industrial era (1800) and  $(1 - \delta_{\ell})$  is the share of CO<sub>2</sub> emissions remaining in atmosphere  $\ell$  periods ahead. Higher concentrations of carbon dioxide rise the global radiative forcing,  $F_{t+1}$ , (net inflow of energy), which is approximated as in [Myhre et al. \(1998\)](#), so

$$F_{t+1} = \varphi \log_2(S_{t+1}/S_{\text{pre-ind}}) + F_{t+1}^x \quad (19)$$

where  $\varphi$  denotes the forcing sensitivity, that is, the increase in radiative force when carbon stock doubles with respect to its pre-industrial level.  $F_t^x$  denotes radiative forcing from non-CO<sub>2</sub> greenhouse gases (methane, nitrous oxide, among others). When the inflow of energy from the Sun exceeds the outflow of energy exiting the planet, global temperature rises, according to a process defined by

$$T_{t+1} = T_{\text{pre-ind}} + \sum_{\ell=0}^{\infty} \zeta_{\ell} F_{t+1-\ell}, \quad (20)$$

where  $T_{\text{pre-ind}}$  denotes worldwide temperature over land in the pre-industrial era and  $\zeta_{\ell}$  is the current temperature response to an increase in radiative force  $\ell$  periods ago.

Carbon emissions disseminate in the world quickly and affect global temperature, not local temperatures directly. This is why carbon emissions are a global externality. However, given that we want to quantify our model at a fine geographical resolution, we need to take a stand on the evolution of local temperature in response to changes in global temperatures. We follow [Mitchell \(2003\)](#), who argues that a linear down-scaling relationship provides accurate results.<sup>11</sup> In particular, we let

$$T_t(r) - T_{t-1}(r) = g(r) \cdot (T_t - T_{t-1}), \quad (21)$$

where the coefficient  $g(r)$  tells us by how much, in °C, temperature in cell  $r$  changes when global temper-

---

<sup>11</sup>More precisely, [Mitchell \(2003\)](#) finds small non-linearities in the local climate response to the length of time over which warming has occurred, to the rate at which it has occurred, and to the extent to which global temperature has stabilized. Incorporating these non-linearities has only a negligible effect on our results.

ature changes by one °C. The coefficients  $g(r)$  depend on local physical characteristics of a location, so we keep them fixed over time.

## 2.5 Competitive Equilibrium and Balanced Growth Path

Together the conditions defined above define a dynamic competitive equilibrium of our model. We can show that the system of equations that defines a spatial equilibrium in a given period can be reduced to a system of equations for population and wages in each location. All other variables, including firm investments, can then be directly computed using the equations presented above. We summarize this result in the following lemma.

**Lemma 1.** *For any  $t$  and for all  $r \in S$ , given  $CumCO2_{t-1}$ ,  $L_t$ ,  $T_t(\cdot)$ ,  $\bar{b}_t(\cdot)$ ,  $\bar{a}_t(\cdot)$ ,  $\varsigma(\cdot, \cdot)$ ,  $m(\cdot, \cdot)$  and  $H(\cdot)$ , the equilibrium energy price  $\mathcal{Q}_t(\cdot)$ , wage  $w_t(\cdot)$ , population density  $L_t(\cdot)$  and utility  $u_t(\cdot)$  schedules satisfy equations (3), (4), (9), (11), (12) as well as the system of equations*

$$w_t(r) = \bar{w}_t(r)^{\frac{1}{1+2\theta}} L_t(r)^{\frac{\alpha-1+\theta(\lambda+\gamma_1/\xi-(1-\mu))}{1+2\theta}} \mathcal{Q}_t(r)^{-\frac{(1-\chi)\mu}{1+2\theta}} H(r)^{-\frac{1}{1+2\theta}} \left( \frac{\bar{b}_t(r)}{u_t(r)} \right)^{-\frac{\theta}{1+2\theta}},$$

$$\left( \frac{\bar{b}_t(r)}{u_t(r)} \right)^{-\theta} L_t(r)^{-\lambda\theta} w_t(r)^{-\theta} = \kappa_1 \left( \int_S \bar{a}_t(v) L_t(v)^{\alpha-(1-\mu-\gamma_1/\xi)\theta} \mathcal{Q}_t(r)^{-(1-\chi)\mu\theta} w_t(r)^{-\theta} \varsigma(r, v)^{-\theta} dv \right),$$

where  $\kappa_1$  is a time-invariant constant and the climatic variables  $E_t^f$ ,  $CumCO2_t$ ,  $S_{t+1}$ ,  $F_{t+1}$ ,  $T_{t+1}$ ,  $T_{t+1}(\cdot)$  are computed from equations (10), (18), (19), (20) and (21).

The proof the Lemma 1 is relegated to Appendix A.1 and parallels results in Desmet et al. (2018). Furthermore, we can show that there exists a unique solution to the system in Lemma 1 if (i)  $\epsilon = 1$  or  $v^f = v^c$ , and (ii)  $\frac{\alpha}{\theta} + \frac{\gamma_1}{\xi} \leq \lambda + (1 - \mu) + \Omega$ . The first condition requires that either the elasticity of substitution between fossil fuels and clean energy is one (Cobb-Douglas) or the innovation elasticity with respect to global real income growth is the same across energy types. Those assumptions allows us to keep the log-linear structure of the model.<sup>12</sup> The second condition is identical to the one in Desmet et al. (2018). It states that the static agglomeration economies associated with the local production externalities,  $\alpha/\theta$ , and the degree of returns to innovation,  $\gamma_1/\xi$ , do not dominate the three congestion forces. These three congestion forces are governed by the value of the negative elasticity of amenities to density,  $\lambda$ , the share of land in production which determines the degree of local decreasing returns,  $1 - \mu$ , and the variance of taste shocks,  $\Omega$ .

A spatial equilibrium in a given period determines firm innovation, energy use, and carbon emissions. Hence we can use equations (2), (7), and the climate and carbon cycle model, to determine temperatures and next period's amenities and productivities. This allows us to compute the dynamic equilibrium forward, period by period, for as many years as needed. As we show in Appendix A.3, eventually the distribution

<sup>12</sup>In the model quantification below, our baseline parametrization deviates from this condition slightly, but numerically we find that the solution is robust to a variation in initial conditions.

of population across space and the world real output growth rate converge to a balanced growth path if: (i) total natality rates  $1 + n_t(r)$  converge to one as income per capita grows; (ii) the stock of carbon is finite, and  $(1 - \delta_\ell)$ ,  $\zeta_\ell$ ,  $E_\ell^x$  and  $F_\ell^x$  converge to constant values, so eventually temperatures stabilize; (iii)  $\epsilon = 1$  or  $v^f = v^c$ ; and (iv)  $\frac{\alpha}{\theta} + \frac{\gamma_1}{\xi} + \frac{\gamma_1}{\xi(1-\gamma_2)} \leq \lambda + (1 - \mu) + \Omega$ . The last condition, which is identical to the one in [Desmet et al. \(2018\)](#), states that agglomeration forces, that now include also dynamic agglomeration forces through innovation,  $\frac{\gamma_1}{\xi(1-\gamma_2)}$ , are weaker than the three congestion forces. The dynamics of the model are very protracted, so convergence to a balanced growth path is not fully achieved for the four-century horizon that we consider. We now proceed to quantify our model.

### 3 Quantification

We quantify the model at the  $1^\circ$  latitude by  $1^\circ$  longitude spatial resolution, which is the spatial resolution of the G-Econ dataset. Our baseline year is 2000. In order to quantify the model we need values for all the economy-wide parameters, plus location specific values for initial fundamental amenities, productivities, and migration costs, as well as bilateral transport costs. We also need to parametrize the extraction cost of fossil fuels, estimate the damage functions on amenities, productivities, and natality rates, and quantify the carbon cycle and climate module.

We follow the quantification strategy in [Desmet et al. \(2018\)](#) for the common parts of the model. Table 1 summarizes the parameter values used in the baseline case. Local fundamental amenities and productivities are recovered so that the model matches exactly population and income in 2000. Migration costs are recovered so that the model matches exactly the observed change in population between 2000 and 2005. All these local characteristics are exactly identified by an inversion procedure described in detail in [Desmet et al. \(2018\)](#). Bilateral trade costs are based on optimal routing using the fast marching algorithm. In what follows, we describe the estimation of three families of parameters and functions, namely, the evolution of energy prices; the construction of the damage functions on amenities, productivities, and natality rates; and the carbon cycle, as well as the climate and the down-scaling factors. Appendix B provides details on the data used in the quantification.

#### 3.1 Energy Prices

We split the estimation of the energy component in four steps. First, we parametrize the cost of extracting fossil fuels  $f(\cdot)$  from the ground. Second, we calibrate the energy share in production,  $\mu(1 - \chi)$ , and the share of fossil fuels in the energy aggregator,  $\kappa$ . Third, we construct prices for fossil fuels and clean energy at the cell level for the year 2000 and retrieve the initial level of the productivities  $\zeta_0^f(\cdot)$ ,  $\zeta_0^c(\cdot)$ . Finally, we set  $v^f, v^c$  to match historical data on global  $\text{CO}_2$  emissions and clean energy use.

To estimate the cost of extracting fossil fuels  $f(\cdot)$ , we employ estimates from [Rogner \(1997\)](#) and [Bauer et al. \(2017\)](#). To construct quantity-cost relations for fossil fuel resources, [Rogner \(1997\)](#) analyzed histor-



1. Energy: $q_t^\omega(r) = \phi_t^\omega(r)^{\gamma_1} z_t^\omega(r) (L_t^\omega(r)^\chi e_t^\omega(r)^{1-\chi})^\mu$ , $e_t^\omega(r) = (\kappa e_t^{f,\omega}(r)^{\frac{\epsilon-1}{\epsilon}} + (1-\kappa)e_t^{c,\omega}(r)^{\frac{\epsilon-1}{\epsilon}})^{\frac{\epsilon}{\epsilon-1}}$ $Q_t^f(r) = f(CumCO2_t)/\zeta_t^f(r)$ , $Q_t^c(r) = 1/\zeta_t^c(r)$ , $\zeta_t^j(r) = (y_t^w/y_{t-1}^w)^{v^j} \zeta_{t-1}^j(r)$	
$\chi = 0.957$	Relation between global GDP, CO <sub>2</sub> emissions flow and price
$\epsilon = 1.6$	Elasticity of substitution (Popp (2004); Papageorgiou et al. (2017))
$\kappa = 0.89$	Relation between prices and quantities of fossil fuels and clean energy
$f(\cdot)$	Extraction costs (Rogner (1997); Bauer et al. (2017))
$\zeta_0^f(\cdot), \zeta_0^c(\cdot)$	Target current cell-level energy use
$v^f = 0.95$	Target historical global CO <sub>2</sub> emissions
$v^c = 1.05$	Target historical global clean energy use
2. Damage functions: $\Lambda^a(\Delta T_t(r), T_t(r))$ , $\Lambda^b(\Delta T_t(r), T_t(r))$ , $n_t(r) = \eta(y_t(r), L_t(r))$	
$\Lambda^a(\cdot), \Lambda^b(\cdot)$	Relation between temperature and productivities and amenities
$\eta(\cdot)$	Relation between real GDP and temperature and natalities
3. Carbon cycle and climate	
$g(\cdot)$	IPCC (2013) and statistical down-scaling
4. Preferences: $\sum_t \beta^t u_t(r)$ , $u_t(r) = (1 + \Lambda_t^b(r)) \bar{b}_{t-1}(r) L_t(r)^{-\lambda} [\int_0^1 c_t^\omega(r)^\rho d\omega]^{1/\rho}$ , $u_0(r) = e^{HDI_0(r)^3/\psi}$	
$\beta = 0.965$	Discount factor
$\rho = 0.75$	Elasticity of substitution of 4 (Bernard et al. (2003))
$\lambda = 0.32$	Relation between amenities and population (Desmet et al. (2018))
$\Omega = 0.5$	Elasticity of migration flows wrt income (Monte et al. (2018))
$\psi = 0.05$	Relation between utility and HDI (Kummu et al. (2018))
5. Technology: $q_t^\omega(r) = \phi_t^\omega(r)^{\gamma_1} z_t^\omega(r) (L_t^\omega(r)^\chi e_t^\omega(r)^{1-\chi})^\mu$ , $F_{r,t}^\omega(z) = e^{a_t^\omega(r)z^{-\theta}}$ , $a_t^\omega(r) = \bar{a}_t(r) L_t(r)^\alpha$	
$\alpha = 0.06$	Static elasticity of productivity to density (Carlino et al. (2007))
$\theta = 6.5$	Trade elasticity (Eaton and Kortum (2002); Simonovska and Waugh (2014))
$\mu = 0.8$	Non-land share in production (Greenwood et al. (1997); Desmet and Rappaport (2017))
$\gamma_1 = 0.319$	Relation between population distribution and growth (Desmet et al. (2018))
6. Productivity evolution: $\bar{a}_t(r) = (1 + \Lambda_t^a(r)) \left( \phi_{t-1}(r)^{\theta\gamma_1} [\int \bar{a}_{t-1}(v) dv]^{1-\gamma_2} \bar{a}_{t-1}(r)^{\gamma_2} \right)$ , $\varphi(\phi) = \nu \phi^\xi$	
$\gamma_2 = 0.993$	Relation between population distribution and growth (Desmet et al. (2018))
$\xi = 125$	Desmet and Rossi-Hansberg (2015)
$\nu = 0.15$	Initial growth rate of real GDP of 1.75%
7. Trade costs	
$\varsigma(\cdot, \cdot)$	Allen and Arkolakis (2014) and Fast Marching Algorithm
8. Migration costs	
$m_2(\cdot)$	Match population change between 2000 and 2005 (Desmet et al. (2018))

Table 1: Summary of parametrization.

ical marginal production costs for different fossil fuel deposits and found a stable relation across regions and time: extraction costs are flat when resources are abundant, but they rise sharply as the resource gets exhausted.<sup>13</sup> Bauer et al. (2017) extend the work of Rogner (1997) and formulate a database of fossil fuel quantities and extraction costs, taking into account different technological, political and economic conditions. We consider the scenario that closest resembles the most pessimistic scenario (RCP 8.5) of the IPCC (2013).<sup>14</sup> Figure 1 displays, in green, the estimates by Bauer et al. (2017) as a function of cumulative CO<sub>2</sub> emissions. We specify the extraction cost function  $f(\cdot)$  as

$$f(CumCO2_t) = \left( \frac{f_1}{f_2 + e^{-f_3(CumCO2_t - f_4)}} \right) + \left( \frac{f_5}{maxCumCO2 - CumCO2_t} \right)^3, \quad (22)$$

where  $CumCO2_t$  denotes the cumulative CO<sub>2</sub> extracted up to period  $t$  and the parameter  $maxCumCO2$  denotes the total stock of carbon dioxide available to produce energy in the planet. We set the value of  $maxCumCO2$  to equalize the cumulative flow of CO<sub>2</sub> for the next five centuries in the most pessimistic scenario (RCP 8.5) of the IPCC (2013), that is 19,500 GtCO<sub>2</sub>.<sup>15</sup> The rest of the parameters are chosen to fit the estimates of Bauer et al. (2017). The black curve in Figure 1 displays the estimated extraction curve, which is increasing and convex.

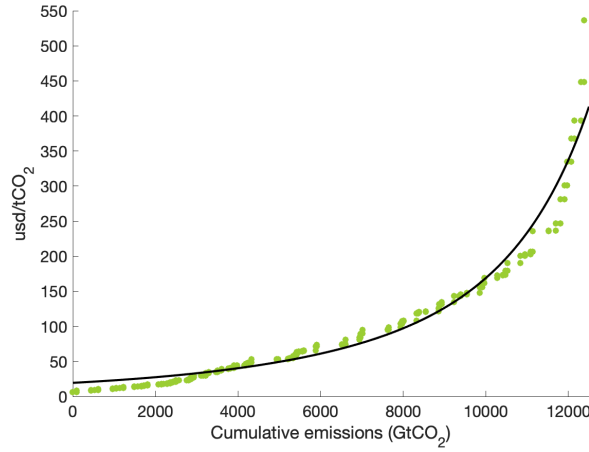


Figure 1: The extraction cost function  $f(\cdot)$ .

We calibrate the parameters  $\chi$  and  $\kappa$  using the first order conditions of the firm's profit maximization. In particular, since technology is Cobb-Douglas, the world's average relative expenditure in fossil fuels and

<sup>13</sup>Drilling costs in the oil and gas industry increase drastically with depth and coal mining is highly sensitive to the characteristics of deep lying coal seams.

<sup>14</sup>Specifically, Bauer et al. (2017) present estimates for five Socio Economic Share Pathways (SSP), which consider different assumptions for the evolution of the world economy. We choose the scenario SSP5 (development based on fossil fuels), which is the one closest to RCP 8.5, and aggregate the costs of coal, natural gas, and oil into a single fossil fuel in terms of tCO<sub>2</sub> per usd.

<sup>15</sup>In comparison, Bauer et al. (2017) consider a smaller total stock of carbon dioxide of 12,550 GtCO<sub>2</sub> and Mcglade and Ekins (2015) of 14,666 GtCO<sub>2</sub>. Appendix F.5 presents results with a variety of alternative values for the total stock of carbon.

clean energy, and the ratio of energy expenditures to the wage bill, are constants given by

$$\left(\frac{Q_0^f}{Q_0^c}\right) \left(\frac{E_0^f}{E_0^c}\right)^{\frac{1}{\epsilon}} = \frac{\kappa}{1-\kappa}, \quad \text{and} \quad \frac{w_0 Q_0 E_0}{w_0 L_0} = \frac{\mu(1-\chi)}{\mu + \gamma_1/\xi}. \quad (23)$$

We take the elasticity of substitution  $\epsilon$  from [Papageorgiou et al. \(2017\)](#) and [Popp \(2004\)](#), who consider a value of 1.6 and obtain global labor income from G-Econ database, so  $w_0 L_0 = 46.6$  trillion usd for the year 2000. We construct the global price of fossil fuels by aggregating the price of coal, natural gas, and oil as in [Golosov et al. \(2014\)](#).<sup>16</sup> This procedure yields an estimate for the price of fossil fuels of  $w_0 Q_0^f = 78.22$  usd/tCO<sub>2</sub>. [Acemoglu et al. \(2019\)](#) estimate the price of clean energy to be 1.15 times that of natural gas. We use that relation to obtain a price of 249.90 usd per ton of oil equivalent (toe). In turn, one ton of oil equivalent generates 2.8466 tons of CO<sub>2</sub>, which is the weighted average of carbon intensities of coal, oil, and natural gas for the year 2000. With those prices and considering that the use of energy from fossil fuels is  $E_0^f = 8.88$  Gtoe ([IPCC \(2013\)](#)) and from clean sources is  $E_0^c = 1.23$  Gtoe ([BP \(2019\)](#)) we obtain  $\kappa = 0.89$  and  $\chi = 0.96$ .<sup>17</sup>

The next step is to measure the productivity of dirty  $\zeta_0^f(\cdot)$  and clean energy  $\zeta_0^c(\cdot)$  in the initial period for each cell. To do so we use the first order conditions of the firm's optimization problem in each cell, together with equation (9), to obtain

$$\zeta_0^f(r) = \left(\frac{\mu + \gamma_1/\xi}{\mu(1-\chi)\kappa}\right) \left(\frac{e_0(r)}{L_0(r)}\right) \left(\frac{e_0^f(r)}{e_0(r)}\right)^{\frac{1}{\epsilon}} f(CumCO2_0), \quad (24)$$

and

$$\zeta_0^c(r) = \left(\frac{\mu + \gamma_1/\xi}{\mu(1-\chi)(1-\kappa)}\right) \left(\frac{e_0(r)}{L_0(r)}\right) \left(\frac{e_0^c(r)}{e_0(r)}\right)^{\frac{1}{\epsilon}}. \quad (25)$$

Labor at the cell-level is directly taken from the G-Econ database. To construct cell-level energy use of fossil fuels and clean energy, we first start with data for CO<sub>2</sub> emissions and clean energy use at the country-level from [BP \(2019\)](#), [Crippa et al. \(2019\)](#) and [IEA \(2019\)](#). Then, we allocate energy use across cells within countries using the share of emissions in the Emissions Database for Global Atmospheric Research (EDGAR).

Finally, to estimate the elasticity of technology in the fossil fuel sector,  $v^f$ , and in the clean energy

---

<sup>16</sup>[Golosov et al. \(2014\)](#) propose that energy from fossil fuels is a CES composite of coal, natural gas, and oil, with elasticity of substitution of 1.11, which corresponds to the unweighted average of the elasticity of substitution between coal and oil, coal and natural gas, and oil and natural gas, according to [Stern \(2012\)](#). [Acemoglu et al. \(2019\)](#) focus on the electricity sector and consider an elasticity of substitution of 2, in line with [Bosetti et al. \(2007\)](#), so that fossil fuels are more substitutable between them than with respect to clean energy. The representative prices of oil, natural gas and coal are the average of the Brent, U.S. Henry Hub, and U.S. Central Appalachian, respectively, over the period 1983-2017 to smooth short-run fluctuations. Data on prices is taken from [BP \(2019\)](#) and data on quantities from [IEA \(2019\)](#).

<sup>17</sup>This parametrization implies that the energy share in production is 3.3%, which is slightly smaller than the values used in the literature, where [Golosov et al. \(2014\)](#) use 4%, [Hassler et al. \(2019\)](#) 5.55%, and [Krusell and Smith \(2017\)](#) 6%.

sector,  $v^c$ , with respect to global real GDP growth, we construct historical global CO<sub>2</sub> emissions and clean energy use from IEA (2019) and BP (2019). We then run the model backwards in time for 50 periods and find the elasticities that provide the best fit of the historical data on relative energy use. The resulting elasticity for clean energy is larger than the one for fossil fuels since its use has expanded faster over time ( $v^c = 1.05 > 0.95 = v^f$ ).<sup>18</sup>

### 3.2 The Effect of Local Temperature on Amenities and Productivities

To estimate the damage functions  $\Lambda^a(\cdot)$  and  $\Lambda^b(\cdot)$ , which determine how temperature affects the fundamentals of the economy, we first need to compute fundamental amenities and productivity in each location by *inverting the model*. The inversion of the model requires solving the system of equations in Lemma 1 for  $\bar{b}_t(r)$  and  $\bar{a}_t(r)$  using data on wages and population, as well as the data on the amount of land in each cell, and the energy prices we described in the previous section.<sup>19</sup> We can do so for the four periods of data available in G-Econ, namely, 1990, 1995, 2000 and 2005.<sup>20</sup>

The model inversion exactly identifies  $\bar{a}_t(r)$  and  $\bar{b}_t(r)/u_t(r)$ , but is unable to separate  $\bar{b}_t(r)$  apart from  $u_t(r)$ . Intuitively, we cannot identify the numerator from the denominator since, if we observe many individuals in a poor location, it could be because amenities are high or because individuals are trapped there even though utility is very low. To disentangle a location's amenities from its initial utility, we require a measure of utility.<sup>21</sup> Desmet et al. (2018) use as utility measure a subjective well-being survey from the Gallup World Poll. However, this data is only available for one period and only at the country-, rather than cell-level. Thus, we use the Human Development Index (HDI) as our measure of  $u_t(r)$  after transforming it into a cardinal measure of well-being that is linear in log-real income, as in our model.<sup>22</sup>

Once we compute the fundamentals that rationalize the observable data on wages, population and energy prices, we identify the causal effect of temperature on amenities and productivities using a panel fixed effects empirical specification, with temperature entering the regression in a flexible non-parametric way. Our main empirical specification is given by

$$\log(x_t(r)) = \sum_{j=1}^J \delta_j^x \cdot T_t(r) \cdot \mathbb{1}\{T_t(r) \in \mathcal{T}_j\} + \delta^z \cdot Z(r) + \iota(b) + \iota(s) + \varepsilon_t(r) \quad (26)$$

<sup>18</sup>Appendix A.4 outlines the system of equations that solve the model backwards in time and Appendix D describes, in further detail, the estimation of these elasticities.

<sup>19</sup>Appendix A.2 describes the inversion of the model in more detail.

<sup>20</sup>An alternative approach that would give us a longer time series would be to employ data on production from Kummu et al. (2018). This dataset spans a longer period of time, from 1990 to 2015 at a yearly frequency, but it displays a coarser geographical resolution with around 700 sub-national units.

<sup>21</sup>Once we identify  $\bar{b}_t(r)$ , we can obtain the migration costs in order to match the model-implied net migration flows with the ones observed in the data

<sup>22</sup>Appendix C.1 describes the details of this calculation, compares the geography of this index to the measure used in Desmet et al. (2018), and presents corresponding robustness exercises.

where  $x_t(r) \in \{\bar{b}_t(r), \bar{a}_t(r)/\phi_t(r)\}$  are the fundamental amenities and the ratio of fundamental productivities to innovations at cell  $r$  in period  $t$ . We use the ratio  $\bar{a}_t(r)/\phi_t(r)$  in order to account for the effect of endogenous innovation on fundamental productivity over time. The variable  $T_t(r)$  denotes the average January temperature for locations in the Northern Hemisphere and the average July temperature for locations in the Southern Hemisphere over the last decade. The variable  $\mathbb{1}\{T_t(r) \in \mathcal{T}_j\}$  is an indicator function of temperature  $T_t(r)$  being in interval  $\mathcal{T}_j$ . We partition the distribution of temperatures into  $J = 20$  bins, each comprising 5% of the observed temperature values.<sup>23</sup> Average January or July temperatures over land, respectively, range from  $-50.15^\circ\text{C}$  to  $32.85^\circ\text{C}$ .

The non-parametric specification in (26) accommodates the potential non-linearities and bliss-points in the effect of temperature on these fundamentals. That is, a temperature increase of  $1^\circ\text{C}$  might have different impacts in very cold regions, like Siberia, with respect to very hot places, like the Sahara. Thus, the coefficient of interest  $\delta_j^x$ , which is the semi-elasticity of  $x_t(r)$  with respect to temperature, is allowed to vary according to the level of temperature. This implies that the damage function  $\Lambda^x(\cdot)$  can be expressed as the semi-elasticity  $\delta_j^x$ , evaluated at the current level of temperature, times the change in local temperature, namely,

$$\Lambda^x(\Delta T_t(r), T_{t-1}) = \delta^x(T_t(r)) \cdot \Delta T_t(r). \quad (27)$$

Our specification also incorporates a set of time-invariant controls at the cell-level,  $Z(r)$ , and a set of fixed effects,  $\iota(b)$  and  $\iota_t(s)$ , to alleviate potential omitted variable bias. To the extent that temperature is spatially correlated, any variable not included in the estimation, that is spatially correlated, would appear in the error term and would bias our estimate of the coefficient  $\delta_j^x$ . Hence, we follow Nordhaus (2006) and include a number of geographic attributes as cell-level covariates,  $Z(r)$ . Alternatively, we can partition the gridded map into blocks of size 2 cells by 2 cells, denoted by  $\iota(b)$ . Although a bit more spatially aggregated, this specification captures any time-invariant local characteristic at the 2-cell spatial level. In addition, we consider local regional trends at the sub-national level,  $\iota_t(s)$ .<sup>24</sup> Our preferred specification for the effect of temperature on amenities considers the block time invariant fixed effects  $\iota(b)$  and divides the regions of Europe in countries. Amenities are driven by many local characteristics that are hard to explicitly control for, as well as by differences in national history and cultural differences. Hence, using a flexible set of time-invariant fixed effect and trends is important. To estimate the effect of temperature on local productivity we control for geographic factors,  $Z(r)$ , at a detailed local level and use the slightly broader definition of European regional trends that divides Europe in four large regions. Geographic attributes have a direct im-

<sup>23</sup>We employ decadal rather than yearly temperature to capture the long-run effects of temperature thereby exploiting also cross-sectional variation. We employ January and July, rather than yearly temperatures, because the former exhibits larger variation over space, which allows us to better identify the temperature impact on fundamentals. We perform robustness exercises in Appendix C.3 where we use average temperatures. The results are similar, but the point estimates are noisier.

<sup>24</sup>We use two definitions of sub-national units. We start with the regions defined in Kummur et al. (2018) for the whole world and aggregate those in Europe at the (i) country-level and (ii) at the region level, where we divide Europe in four regions (North, South, West and East).

pact on local productivities in agriculture, but also in other sectors through the availability of raw materials and transportation networks. Broader regional evolution in technology depends on regional specialization rather than national boundaries and so are captured through the many sub-national trends in the world and the four European regions. Appendix C.2 describes the details and presents a number of robustness exercises.

Figure 2 displays the baseline estimates of  $\delta^b(T_t(r))$  and  $\delta^a(T_t(r))$ . We allow for spatially correlated errors as in Conley (1999).<sup>25</sup> The bars in the Figure denote the point estimates, the whiskers the 95% confidence intervals and the solid gray curve a logistic approximation.<sup>26</sup> The dashed gray lines represent the 95% confidence intervals of the logistic curves.<sup>27</sup>

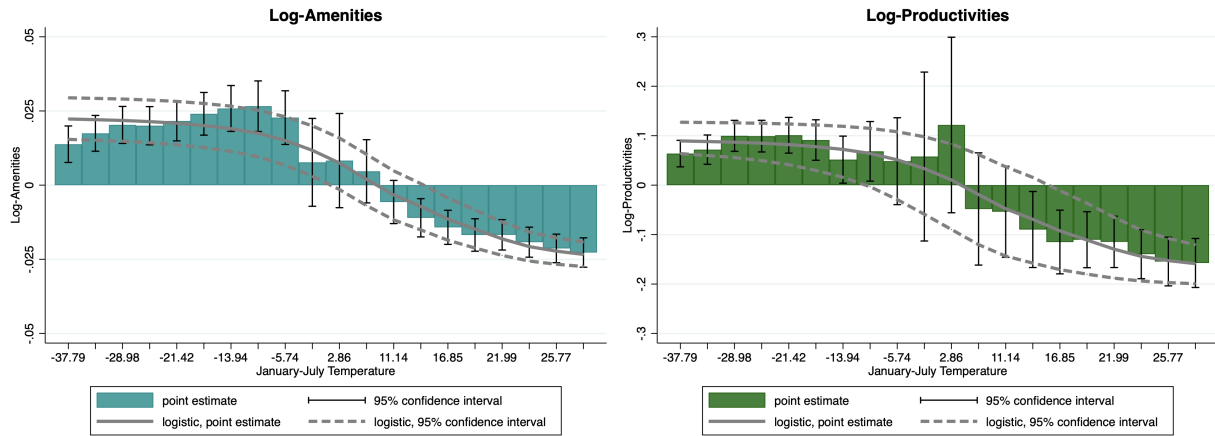


Figure 2: Effect of temperature on fundamental amenities and productivities, using January temperatures for the Northern Hemisphere and July temperatures for the Southern Hemisphere.

As expected, for very cold regions, increases in temperature rise both amenities and productivities. For example, in the coldest bin of January-July temperatures, centered at  $-37.79^{\circ}\text{C}$ , an increase in  $1^{\circ}\text{C}$  augments local amenities by 2.22% and local productivities by 8.94%. In bins with warmer temperatures, the beneficial effects of rising temperatures decline, until they reach zero and eventually turn negative. For January-July temperatures in the warmest bin, centered at  $25.77^{\circ}\text{C}$ , an increase in  $1^{\circ}\text{C}$  reduces local amenities by 2.33% and local productivities by 15.87%. These results highlight the heterogeneous effects of temperature on fundamentals across the range of temperature levels experienced in regions of the world. Extreme temperatures have negative effects and amenities and productivities have bliss-points at moderate ones.

<sup>25</sup>We consider that correlation of errors between cells declines linearly with distance, so that when distance is greater than 550 km (5 cells), correlation vanishes to zero.

<sup>26</sup>We opted for a logistic approximation to be conservative when extrapolating damages to temperatures that are hotter than the ones historically observed. Albouy et al. (2016) and Graff-Zivin and Neidell (2014) argue that individuals reduce their time outdoors as temperatures become uncomfortable, reducing their sensitivity to further temperature changes.

<sup>27</sup>The upper (lower) confidence interval of the logistic curve is constructed using the upper (lower) confidence interval of the point estimates and fitting a logistic curve as well.

Optimal temperatures for fundamentals are given by the temperatures at which  $\delta_j^x = \frac{\partial \log(x_t(r))}{\partial T_t(r)}$  equals zero. For amenities we estimate an optimal temperature of 8.8°C, whereas for productivities of 4.5°C.<sup>28</sup>

### 3.3 The Effect of Income and Temperature on Natality Rates

We specify local natality rates as a function of real income and temperature. In particular, we let

$$n_t(r) = \eta^y(\log(y_t(r))) + \eta^T(T_t(r), \log(y_t^w)),$$

where

$$\eta^y(\log(y_t(r))) = \mathcal{B}(\log(y_t(r)); b^\ell) \cdot \mathbb{1}(\log(y_t(r)) < b^*) + \mathcal{B}(\log(y_t(r)); b^h) \cdot \mathbb{1}(\log(y_t(r)) \geq b^*), \quad (28)$$

with  $\mathcal{B}(\log(y_t(r)); b) = b_0 + b_2 e^{-b_1(\log(y_t(r)) - b^*)^2}$  and

$$\eta^T(T_t(r), \log(y_t^w)) = \frac{\mathcal{B}(T_t(r); b^T)}{1 + e^{b_w[\log(y_t^w) - \log(y_0^w)]}}. \quad (29)$$

The term  $\eta^y(\cdot)$  captures the standard argument in [Becker \(1960\)](#) that, as income grows, household substitutes quantity for quality by investing more in their children. [Delventhal et al. \(2019\)](#) analyze birth and death rates across countries and find that almost all countries in the world have experienced (or are experiencing) a demographic transition, that is, they move from a phase of high to one of low natality. Furthermore, they argue that the start of this transition occurs at roughly the same income level. Hence, the functional form in (28) specifies an inverse and asymmetric bell-shaped function, so that when income is sufficiently low, natality rates are high but, as income grows, natality rates decline until they reach negative values, as evidenced by some rich countries today. To impose that global population is stable in the long-run, natality rates tend towards zero as income rises further.<sup>29</sup>

The relation between temperature and natality is captured by  $\eta^T(\cdot)$ . [Carleton et al. \(2020\)](#) estimate that higher income allows households to adapt to changes in temperature, thereby flattening the mortality response to temperature. [Barreca et al. \(2016\)](#) argue that access to health care, electricity and, particularly, air conditioner have been important adaptation mechanisms. Thus, we specify  $\eta^T(\cdot)$  as a symmetric bell-shaped function, so that when temperatures are extreme, natality rates are low, and they are maximized in temperate climates. Finally, we interact this component with a decreasing function of global income,  $y_t^w$ , to

---

<sup>28</sup>Although the literature estimating the impact of temperature on fundamentals, rather than endogenous outcomes, is scarce, our estimates for optimal temperatures are roughly in line with available studies. [Burke et al. \(2015b\)](#) employ country-level data for the period 1960-2010 and, through panel methods, estimate that economic production is concave in annual temperature peaking at 13°C. [Krusell and Smith \(2017\)](#) consider that a yearly temperature of 11.6°C maximizes productivity and [Nordhaus \(2006\)](#) estimates that the optimal yearly temperature for output lies between 7°C and 14°C. If we translate this range to January-July temperatures, which is the temperature measure we use in our estimation, this range becomes -5°C to 6°C, which includes our bliss-point for productivity.

<sup>29</sup> $\mathcal{B}(\cdot)$  is a bell-shaped function where  $b_0$  and  $b_2 + b_0$  are the minimum and maximum (maximum and minimum) values if  $b_2 > 0$  ( $b_2 < 0$ ),  $b_1 > 0$  governs the slope of the incline and decline, and  $b^*$  is the value that maximizes the function.



account for the remedies that a wealthier world would provide for the effect of temperature on mortality.

In order to estimate the parameters defining the natality rate function,  $b^\ell, b^h, b^T, b_w$ , we run the model backwards for 50 periods and compute the endogenous historical population levels predicted by the model. Thus, we find the coefficients that maximize the model's fit with the country-level historical data on natality rates.<sup>30</sup> Figure 3 displays the resulting functions  $\eta^y(\cdot)$  and  $\eta^T(\cdot)$ . They illustrate the position of the world average, a cold and rich country (United States), and a hot and poor country (Zambia), for the years 1950 and 1999.<sup>31</sup>

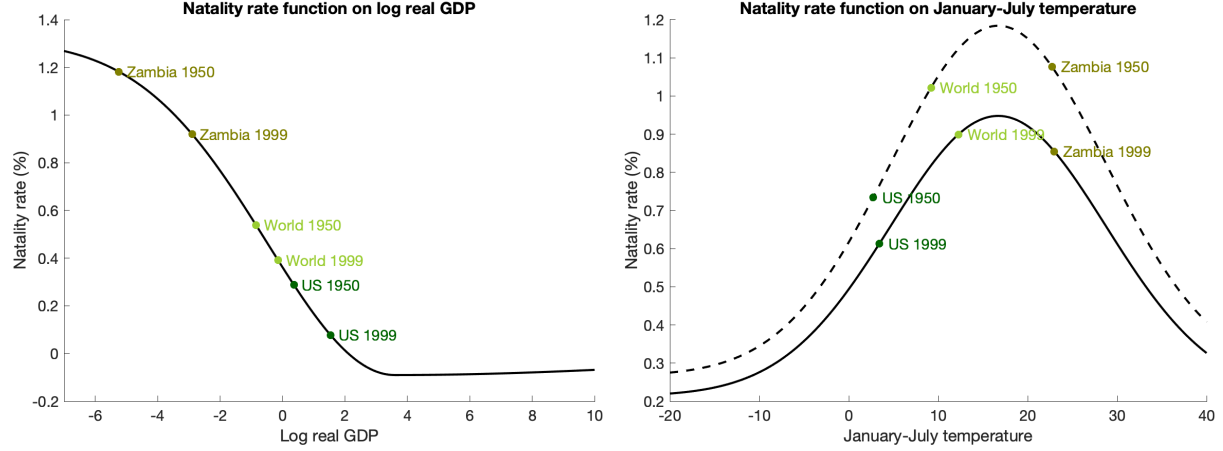


Figure 3: The natality rate function.

Finally, with the the quantified natality rate function, we compute the migration costs  $m_2(\cdot)$  that make the model exactly rationalize the population levels observed in 2005. The procedure to obtain the migration costs is described in detail in Appendix A.5 and the procedure to estimate the natality function, as well as some additional results, are presented in Appendix D.

### 3.4 Carbon Cycle and Temperature Downscaling

We adopt the specification of the carbon cycle and the global climate component proposed by IPCC (2013). We choose parameter values such that the carbon cycle in Section 2.4 exactly reproduces the values displayed in IPCC (2013). The details and exact values used are discussed in Appendix E. As we will show below, the end result will be that the endogenous evolution of temperature in our baseline scenario will reproduce the temperature path of the RCP 8.5 scenario almost exactly.

We use equation (21) to down-scale worldwide temperature at the cell-level. We use the Berkeley Earth Surface Temperature Database, which provides temperature data at a geographic resolution of  $1^\circ \times 1^\circ$ .

<sup>30</sup>We weight countries by population size with additional weight for more recent observations. Additionally, we impose that the natality function  $\eta(\cdot)$  matches the global natality rate in 2000 and 2020. Figures 34 and 33 compare the cross-section of country-level natality rates in 2000 and the historical global natality rates from the data and the estimation, respectively.

<sup>31</sup>1950 and 1999 mark the beginning and end of the time period employed in the estimation of the natality rate function.



In order to obtain a smooth spatial shape of the temperature scaler,  $g(\cdot)$ , we specify it as a function of geographical attributes of each cell. Specifically, as a Chebyshev polynomial of order 10 on latitude and longitude (including a cross term), elevation, distance to the coast, distance to non-frozen oceans, distance to water bodies, vegetation density, share of ice-covered land and albedo.<sup>32</sup> We estimate equation (21) by weighted OLS, with higher weight given to more recent observations.<sup>33</sup> The estimation procedure yields a good fit; it captures 83% of the variation in the local temperature data. Appendix E elaborates further on the construction of the temperature scaler.

Figure 4 plots the local January-July temperatures in 2000 and the temperature scaler for every cell of the world. An increase in global temperature of  $1^\circ\text{C}$  results in increases as large as  $2.2^\circ\text{C}$  close to the north pole, but as low as  $0.5^\circ\text{C}$  in southern locations in Central and South America, Africa, South East Asia, and Australia. Coastal regions tend to experience smaller increases in temperature compared to inland locations. This pattern is attributed to the fact that land absorbs more heat than water. These results are in line with predictions by IPCC (2007). Overall, Figure 4 illustrates the large heterogeneity in the impact of global warming on local temperatures and underscores the importance of a high resolution spatial model.

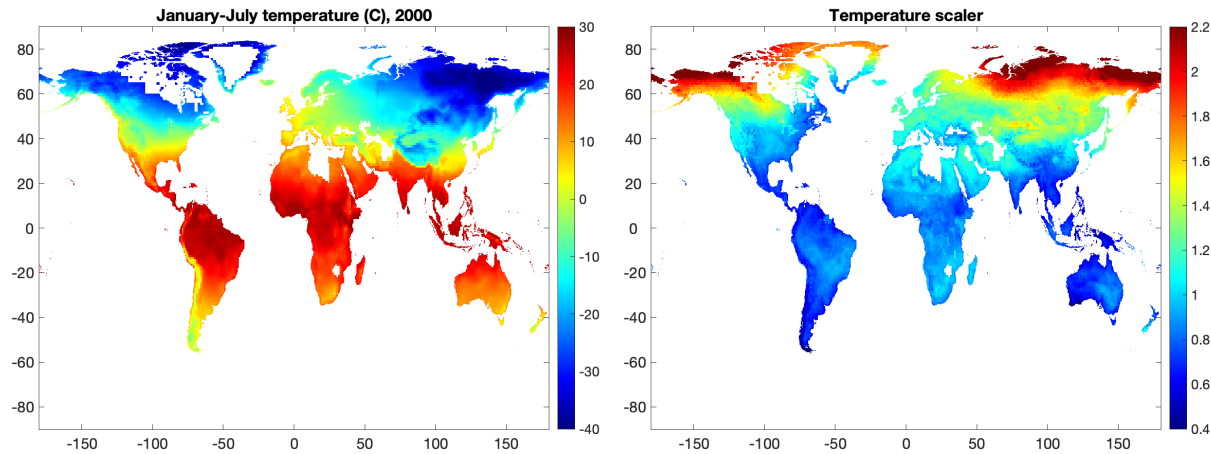


Figure 4: Local January-July temperature in 2000 and temperature scaler.

## 4 The Baseline Scenario

In the baseline scenario we run the quantified model and obtain predictions for 400 years, corresponding to the period 2001 to 2400. This scenario assumes that no new climate policy is put in place and that the evolution of clean technology follows the process described in the previous sections. We organize the exposition of the quantitative results as follows. First, we describe the endogenous evolution of aggregate

<sup>32</sup>Albedo is the ratio of light that a surface reflects compared to the total sunlight it receives. Surfaces that reflect a lot of light are bright and have high albedo. For example, snow has a high albedo, whereas forests have a low albedo.

<sup>33</sup>The weight for year  $t$  is given by  $(2018 - t)^{-1}$ .

CO<sub>2</sub> emissions and average global temperature and compare them with the projections by IPCC (2013). Then, we explore the corresponding evolution of economic outcomes, namely, amenities, productivities, population density, and real GDP. Finally, we run counterfactuals where we eliminate the effect of the rise in temperatures in order to evaluate and decompose the welfare effects of global warming.

#### 4.1 Emissions and Temperature in the Baseline Scenario

Figure 5 presents the path for CO<sub>2</sub> emissions predicted by the model, as well as its comparison with the two most pessimistic scenarios (RCP 8.5 and 6.0) in IPCC (2013). Carbon dioxide emissions from fossil fuel combustion are expected to grow over the current century, since the improvements in productivity (generated by endogenous growth in global real income) overcomes the increase in the relative price of carbon-based energy that results from the larger extraction cost associated with increasing cumulative emissions. CO<sub>2</sub> emissions reach a peak of 116 GtCO<sub>2</sub> in 2110, a value slightly higher than the 106 GtCO<sub>2</sub> of the most pessimistic IPCC scenario. After that point, the flow of carbon dioxide declines towards zero, since extraction costs increase sharply as fossil fuels become exhausted. Note that, although the bell-shaped carbon dioxide emission path is an endogenous outcome, derived from the optimizing behavior of agents, it parallels the exogenous abatement process that makes the emission projections of IPCC (2013) decline eventually.

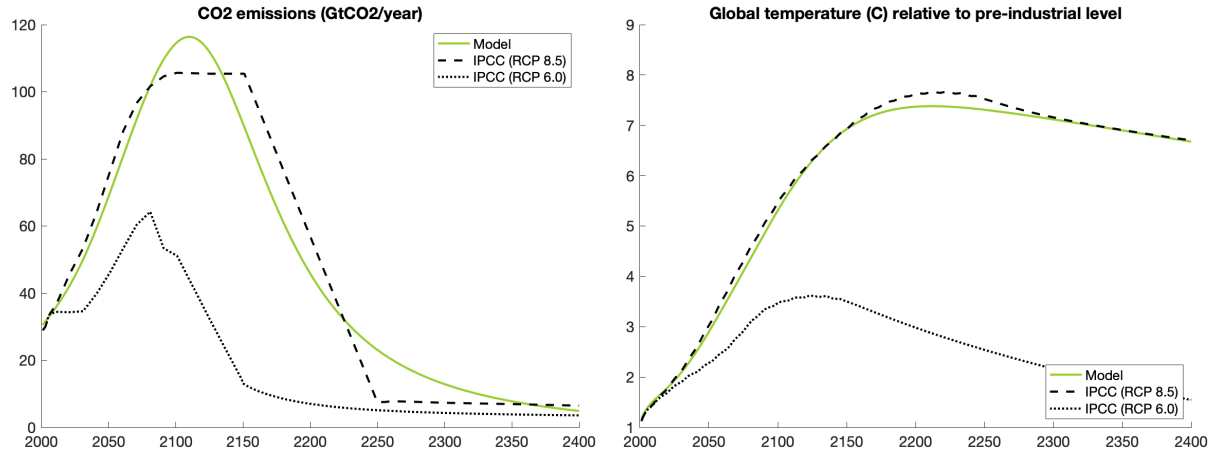


Figure 5: CO<sub>2</sub> emissions and global temperature.

The rise in the concentration of greenhouse gases increases global temperatures, as shown in Figure 5, so that by the end of the current century, global temperature is expected to rise 5.3°C with respect to its pre-industrial level. By 2200 the rise in global temperatures reaches 7.4°C. As carbon dioxide consumption declines towards zero, global temperature approximates its long-run level at between 6 and 7°C above pre-industrial level. As expected, given our parametrization of the carbon cycle and the close match between the emission trajectory in our model and that in the RCP 8.5 scenario, the temperature evolution matches the RCP 8.5 almost exactly.

As illustrated in Figure 4, the increase in global temperatures yields heterogeneous increases in local temperatures across the world. In 2000, only 19.91% of the land surface experienced January-July temperatures higher than 20°C. Two hundred years later this share is predicted to increase to 30.59%, covering most of North and Central Africa, the Middle East, India, Brazil and Central America. At the other extreme, in 2000, 11.18% of the global land surface exhibited January-July temperatures below -30°C, mainly located in North Canada, Greenland, and Northern Russia. This share is expected to decline to 0.45% in 2200.<sup>34</sup>

## 4.2 Local Amenities, Productivity, and Population in the Baseline Scenario

To measure how changes in temperature distort economic outcomes, we compare two scenarios: A factual scenario, our baseline, in which temperature affects fundamental amenities, productivities, and natality rates as described in Section 3, and a counterfactual scenario, in which temperature does not disrupt these fundamentals and, therefore, has no effect on economic outcomes.

Figure 6 shows the ratio of fundamental amenities and productivities in 2200 in the scenario with global warming relative to the counterfactual scenario without global warming. Values greater (lower) than one indicate that temperature changes are predicted to increase (decrease) the respective fundamental characteristic. As we argued before, the estimated temperature damage functions,  $\Lambda^b(\cdot)$  and  $\Lambda^a(\cdot)$ , imply that rises in temperature have differentiated effects over space depending on the level of temperature. In the year 2200, the coldest places in the world experience amenity gains as large as 40%, while the hottest places in the world are projected to suffer amenity losses of 16%. The pattern of changes in amenities depends primarily on latitude, with equatorial regions losing the most, but the geographic patterns are quite rich. Inland regions in Africa, South America, and Australia lose more than what their latitude would predict, as does the U.K., and parts of continental Europe. The average amenity losses, weighted by the 2200 population in the baseline scenario, amounts to 5.1%.

The impact of global warming on fundamental productivities by 2200 exhibits similar patterns, although more pronounced. Note that the effects on productivity are not only driven by the direct impact of temperature on the estimated damage function,  $\Lambda^a(\cdot)$ , but also by endogenous innovation decisions. In parts of Alaska, Northern Canada, Greenland, and Northern Russia productivity doubles relative to the scenario without global warming, and in a few areas the changes in productivity can be even larger. In contrast, in Brazil, Africa, Middle East, India, and Australia we observe declines in productivity of up to 60%. On average, and again weighting by employment in the baseline scenario, world fundamental productivity declines by 19% by 2200 due to rising temperatures.

The geographic configuration of amenities and productivities determines the desirability for residing and producing in particular regions of the world. As the world becomes warmer, the regions where amenities and productivity deteriorate see their population decline. The magnitude of the decline depends on

---

<sup>34</sup>Appendix F.1 presents additional results on the evolution of local temperature over time.

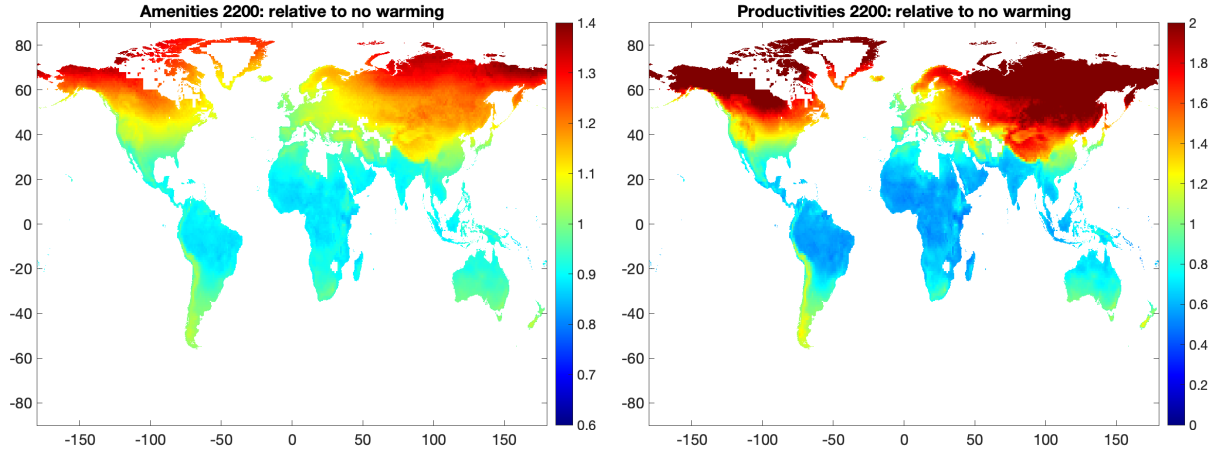


Figure 6: Gains and losses in amenities and productivities from global warming in the year 2200.

natality rates and migration costs, as well as their trade network and other local characteristics. Figure 7 presents population density in 2200 relative to the counterfactual scenario without global warming. Clearly, global warming generates migration towards colder places. Areas to the south of the 30° latitude in the Northern Hemisphere tend to lose population, while areas to the north tend to gain. Most of the developed world (U.S., Europe, and Japan) is just at the boundary and so is not greatly affected. In two centuries, population density in the north of the world is projected to increase by more than 100%, whereas locations close to the Equator are projected to experience declines in population density of roughly 18%. Note that, although inflow migration to the coldest regions is large in relative terms, it is small in absolute terms, since these areas are only sparsely populated. Overall, by 2200, 5.85% of the population resides in a different location due to global warming. More than 600 million people are displaced by this dimension of climate change, namely global warming, alone!

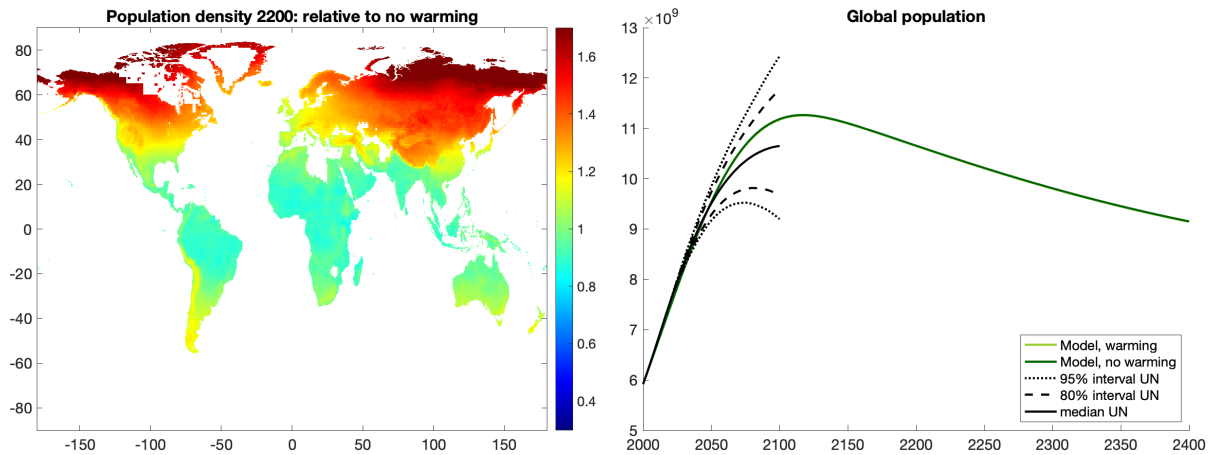


Figure 7: Spatial pattern of population and global population.

Global warming not only affects relocation of population over space, but also its global level. In the

baseline scenario, world population grows until the year 2118, reaching a peak of 11.3 billions inhabitants, as depicted in Figure 7. Afterwards, population declines as the world gets richer and natality rates decline. Since natality rates converge to zero as income grows, global population converges to a stable long-run level. The figure also presents the United Nations global population estimates. The model's population predictions for the first century are somewhat higher than the median estimate by UN (2019), but within the 80% confidence interval. The long-run level of global population estimated by UN (2004) at 9 billions inhabitants is close to our projection in 2400. Global warming has a relatively small impact on world population, the model predicts that higher temperatures lower population in the next 50 years by roughly 31 millions; in the next 100 years by 35 millions; and in the next 200 years by 27 millions.

### 4.3 The Welfare Cost of Global Warming

To evaluate the welfare consequences of global warming, we compute the present discounted value (PDV) of local utility that is not idiosyncratic, namely,  $\sum_{t=0}^{\infty} \beta^t u_t(r)$ . We also present results for the discounted value of real income,  $\sum_{t=0}^{\infty} \beta^t y_t(r)$ . We use a value of the discount factor of  $\beta = 0.965$ .<sup>35</sup> Our choice of the discount factor is restricted by a real output growth rate that is slightly larger than 3% per year. Clearly, to do proper comparisons we need a discount factor for which present discounted values remain finite in all exercises.

Figure 8 displays the spatial distribution of welfare gains, as well as an initial population weighted histogram of the distribution of gains and losses. As before, values smaller than one indicate that the region suffers losses from global warming. The welfare effects of this phenomenon are quite heterogeneous across space. Welfare losses range from 15% in Central and Southern Africa to gains of 14% in the most northern parts of Russia. The right-hand panel of Figure 8 clearly shows that the distribution of damages is bi-modal. The left peak of the distribution, with losses of around 10%, corresponds to India, while the right peak, that experiences small effects, corresponds to parts of China, Europe, Japan, and the U.S. On average, the world is expected to experience welfare losses of 6% in our baseline scenario. As we underscore in the next subsection, there is tremendous uncertainty about the exact level of these aggregate losses, but much less uncertainty about their spatial distribution.<sup>36</sup>

Figure 9 presents losses in the present discounted value of real GDP. The spatial distribution and shape of the histogram are similar than those for welfare. However, the largest losses (7%), largest gains (4%) and standard deviation (0.02) are smaller than those of welfare. This is natural, since the welfare calculation includes the effect of temperature on amenities which intensifies the magnitude and dispersion of climate damages around the world. Furthermore, as we showed in Figure 7, global warming makes people move to locations that have, at least initially, relatively low fundamental amenities.

<sup>35</sup>Appendix F.3 present robustness exercises with respect to the discount factor.

<sup>36</sup>Global average welfare losses are calculated as the population weighted average of the relative present discounted value of utility in the baseline case relative to the counterfactual without global warming.

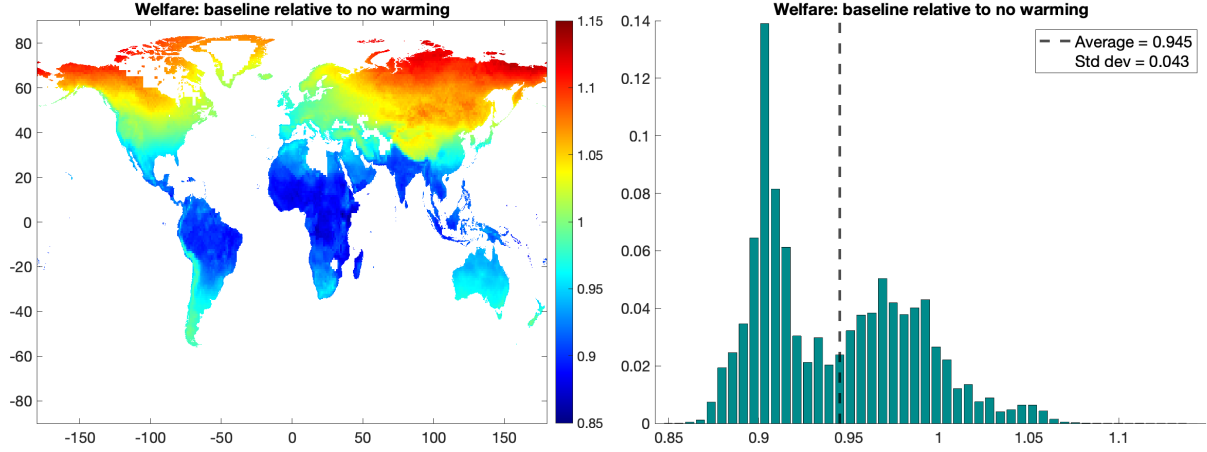


Figure 8: Welfare losses due to global warming.

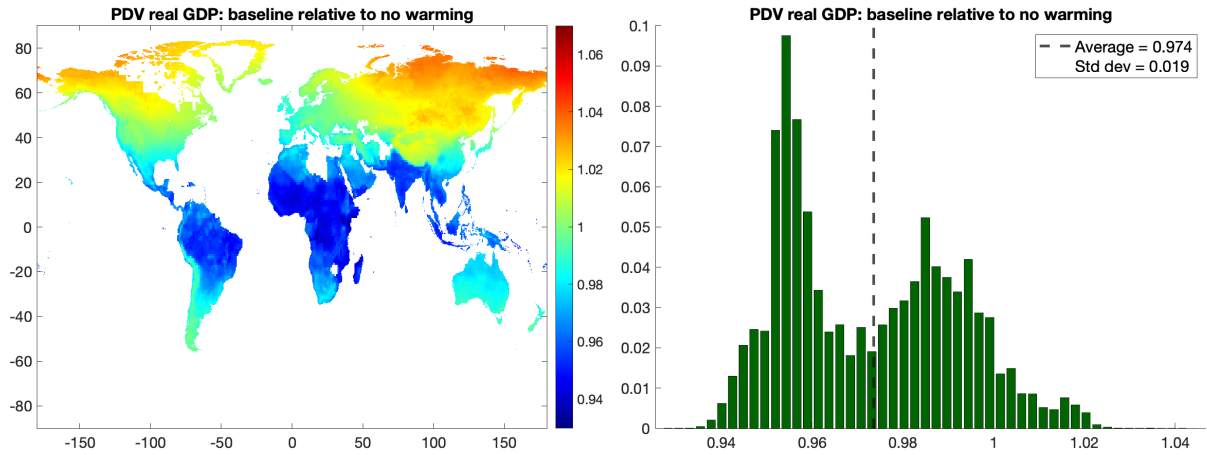


Figure 9: Real GDP losses due to global warming.

#### 4.4 Uncertainty

Our baseline scenario is computed using the logistic fit of the damage coefficients by temperature bin that we estimated in Section 3.2. As we discussed there, although we find evidence of significant temperature effects on amenities and productivity for locations with low and high temperatures, the estimation also yields large confidence intervals. The implied uncertainty embedded in the imprecise estimation of the damage functions translates in uncertainty about the effect that global warming will have on the economy. Of course, we are also uncertain about many of the other parameters of the model as well as about the model specification itself. However, [Desmet et al. \(2018\)](#) perform a number of back-casting exercises that lend credibility to the long-run performance of the economic model and its parametrization. Hence, here we restrict attention to the parametric uncertainty related to the imprecision in the estimation of the coefficients of the temperature damage functions for fundamental amenities and productivities.

Figure 10 presents the global average losses from real GDP and welfare over time in the baseline estima-

tion (solid line) and for damage functions determined by the logistic fit of the boundaries of the different confidence intervals, namely 60%, 80%, 90% and 95%. Baseline damages in real GDP and welfare intensify through the next two centuries, achieving a peak of 4.3% and 9.4%, respectively.<sup>37</sup> Figure 10 illustrates how uncertain we are about the aggregate effect of global warming. The 95% confidence interval includes catastrophic welfare losses of as much as 20% by 2200 but also small global gains. Confidence intervals widen during the first two centuries as temperature increases, but shrink slightly when temperature starts declining.

The large uncertainty on aggregate losses revealed in Figure 10 does not translate into large uncertainty on local relative effects. Figure 11 displays the spatial distribution of real GDP and welfare for the baseline case, the lower 95% confidence interval (i.e. the *worst-scenario*), and the upper 95% confidence interval (i.e. the *best-scenario*). The level of the distributions are clearly different. In the worst-scenario, only a negligible part of the population, 0.02%, experiences welfare gains. Whereas, in the best-scenario, 46.94% of the population undergoes welfare losses. However, the range, standard deviation, and shape of local losses remains roughly similar in all scenarios.<sup>38</sup> This is the sense in which we are less uncertain about relative local effects than about the magnitude of average effects. In the baseline, as well as the best and worst scenarios, the losers from global warming are primarily Central America, Brazil, Africa and India.

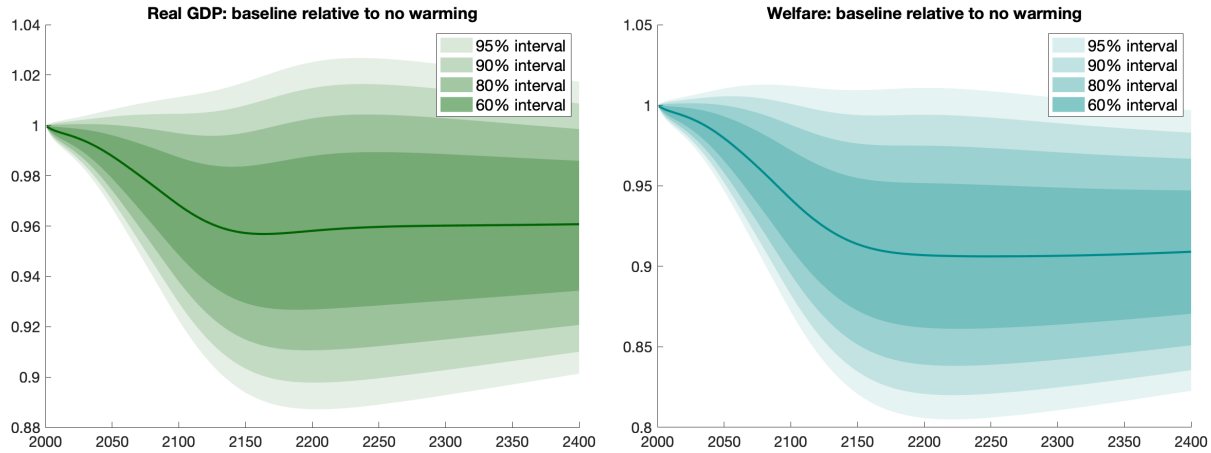


Figure 10: Real GDP and welfare losses over time.

<sup>37</sup>Baseline average damages in real GDP rise until the year 2176. Damages in welfare, in comparison, keep increasing, although mildly, since the damage function on amenities has a greater slope than that of productivities for relatively warm temperatures and population keeps moving to locations with relatively low fundamental amenities.

<sup>38</sup>As we move to more optimistic scenarios, the standard deviation of welfare losses tends to augment slightly. This is the result of the shape of the damage functions on amenities and productivities across different confidence levels. In the most pessimistic scenario, marginal damages seem to be roughly constant in the hottest bins while they are declining in the most optimistic scenarios, as shown in Figure 2.



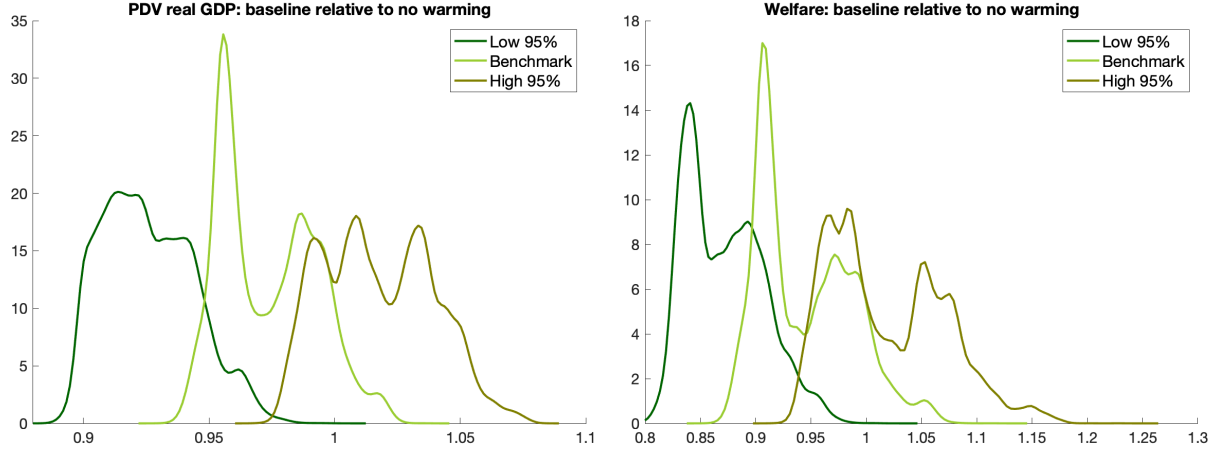


Figure 11: Distribution of Real GDP and welfare losses by uncertainty level.

#### 4.5 Decomposing the Losses from Global Warming by Source

As we have argued above, the two main direct channels through which global warming affects economic outcomes are the effects of changes in temperatures on amenities and productivities. In fact, incorporating the effect of temperature on amenities at this level of spatial disaggregation is, we believe, novel to our study. To understand the contribution of each of these two sources of economic effects, we decompose the warming damages as those arising exclusively from the effect of temperature on local amenities and those arising exclusively from the effect of temperature on local productivities. That is, we calculate two additional counterfactual scenarios setting each of the damage functions to zero for every period and cell, respectively.

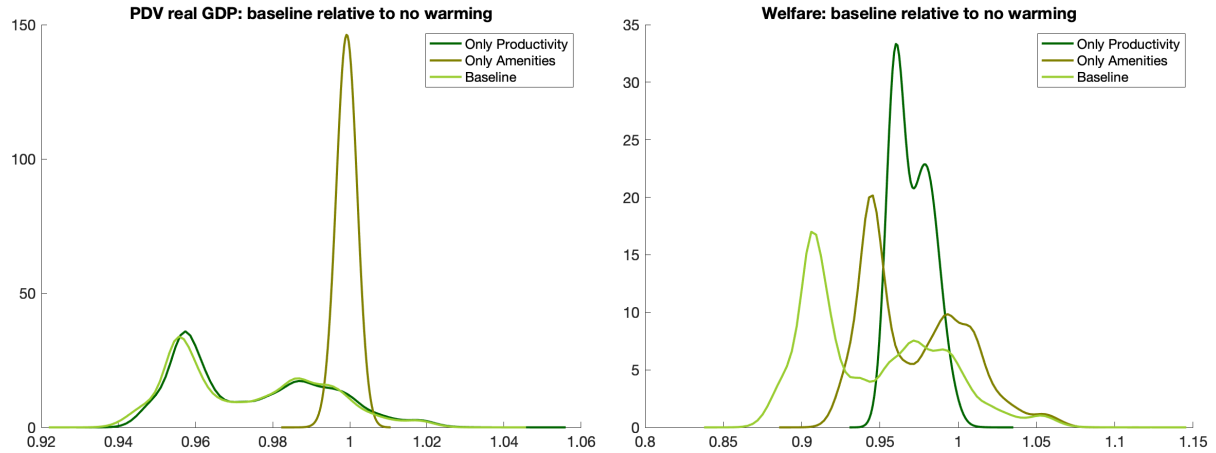


Figure 12: Distribution of Real GDP and welfare losses by damage source.

Figure 12 compares the cross-section of losses in the PDV of real GDP and welfare across damage sources. The spatial distribution of real GDP losses is mainly driven by the productivity component. The



amenity component affects real GDP through its effect on the spatial distribution of population and the corresponding effects of investment. However, the effects are small compared to the direct impact of productivity. In contrast, when we analyze the cross-sectional distribution of welfare, the role of amenities is very large and governs the overall shape of the distribution. For welfare, the productivity component is more uniform across regions with implied losses for almost all locations. This exercise highlights the importance of incorporating the effect of changes in temperature on amenities when assessing the local welfare impact of global warming.

Figure 13 displays the spatial composition of losses in welfare when the damage function only takes into account damages on amenities or productivities, respectively. The large dispersion in the effect coming exclusively from amenities implies large gains in Russia, Canada, and Alaska, and losses in South America, Africa, and India. In contrast, the spatial distribution of the effects coming exclusively through the productivity channel implies losses in most of the southern regions. All southern regions, including Australia, suffer, and the losses reach further north to Mexico and the Southern part of the U.S., as well as India and China. Clearly, the spatial distribution of the losses from global warming that result from each source are quite different.

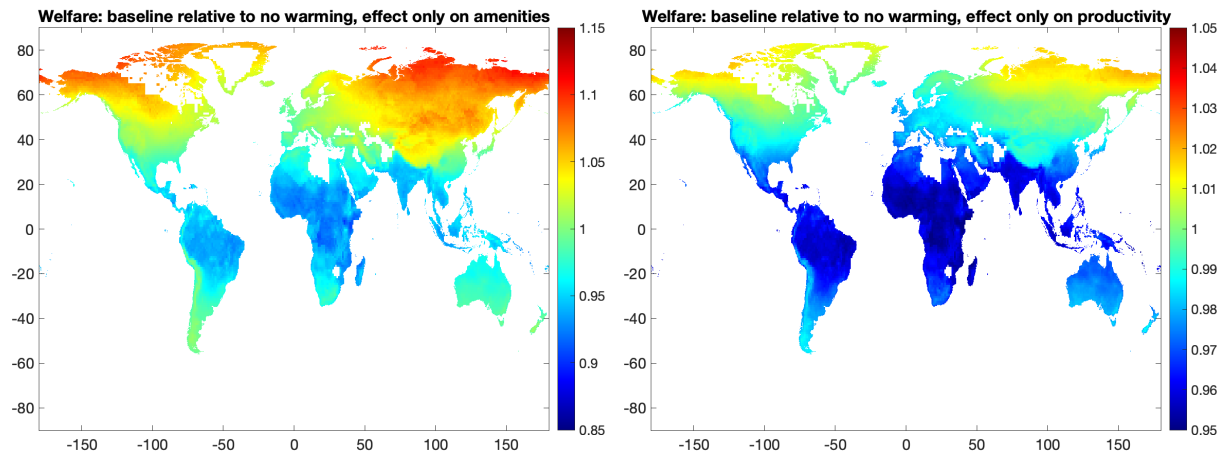


Figure 13: Spatial distribution of real GDP and welfare losses due to global warming by damage source.

To end this section, Figure 14 decomposes the evolution of economic losses over time. When we consider damages on amenities only, cold regions become more amenable for living, which creates an incentive for people to move to some of the most productive places in the world. This migration boosts agglomeration and thus rises global average real GDP slightly for the first 200 years. Eventually, as temperatures decline due to the rising cost of extracting fossil fuels, this process reverses. Welfare, in contrast, exhibits only losses that accelerate as rising temperatures deteriorate amenities in the developing world. When we isolate the damages from warming coming from changes in local fundamental productivity, the evolution of losses in real GDP is similar to the benchmark scenario for the first century. Without the impact of climate on amenities, however, less people move north which results in less agglomeration and slightly larger real

GDP losses. The difference is much larger when considering welfare. The effect on amenities essentially doubles the impact of global warming on welfare throughout. Overall, Figure 14 shows that the effect of temperature on fundamental productivity and the effect of temperature on amenities, each account for about half of the total welfare losses from global warming.

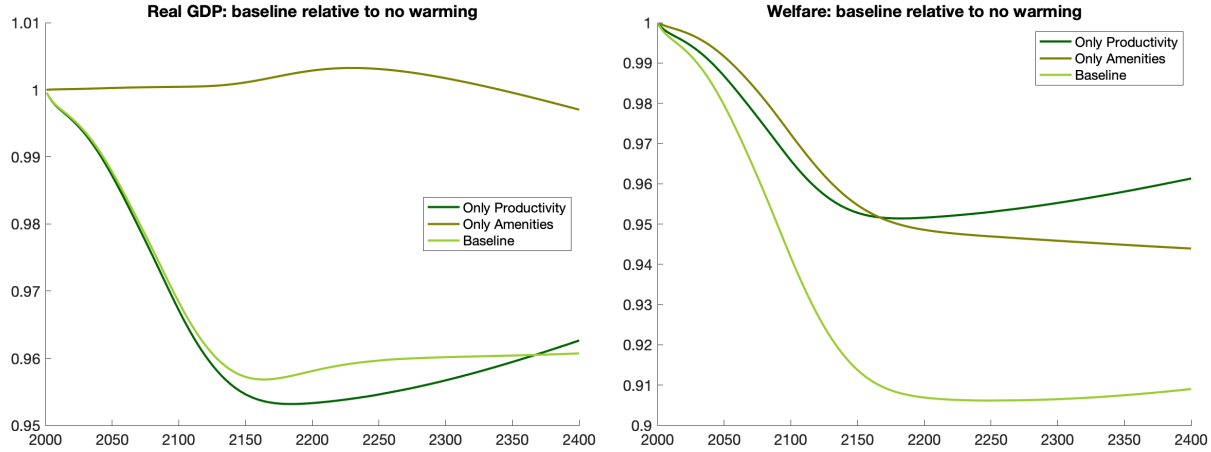


Figure 14: Real GDP and welfare losses by damage source over time.

## 5 Adaptation

In the model we have put forward, agents react to rises in temperatures by moving, trading, and investing in different locations on Earth. These adaptation mechanisms help agents cope with experienced changes in the economic environment. Modelling the effect of global warming using a micro-founded general equilibrium framework that incorporates these mechanisms allows us to incorporate and assess the role of economic adaptation in shaping the economy's response. Of course, the extent to which agents use these adaptation channels depends on their cost. In this section, we evaluate the importance of the different mechanisms by comparing our baseline results with counterfactual scenarios where agents face higher migration, trade, or innovation costs.<sup>39</sup>

### 5.1 Migration

In the baseline scenario we set local migration costs such that the model accounts exactly for the distribution of local population changes between 2000 and 2005. Here, we consider global increases in migration costs by raising the migration cost function  $m_2(\cdot)$  to a power  $\vartheta > 1$ , which corresponds to a proportional increase of size  $\vartheta - 1$  if  $m_2(\cdot)$  is close enough to one. Larger migration frictions imply that agents migrate less to the most productive locations, leading to lower incomes, energy and fossil fuel use, CO<sub>2</sub> emissions, and

<sup>39</sup>Appendix H provides additional details and results.

temperatures. Lower temperatures, in turn, increase productivity and amenities in some locations. In addition, since higher migration costs imply that agents remain in poor locations, and overall incomes are lower, natality rates are higher, leading to increases in population, aggregate fossil fuel consumption, and temperatures. These feedback mechanisms make the effect of migration costs quite complex.

Figure 15 presents the welfare impact of higher migration costs across space and over time. The left panel presents relative welfare with and without global warming in the baseline case with respect to relative welfare with and without global warming in the case with log migration cost that are 25% higher (the diff-and-diff effect of migration costs on the effect of temperature). Red areas in the figure represent locations where larger migration costs make global warming more costly (namely, the baseline better). Clearly, higher migration costs hurt northern regions that tend to benefit from temperature rises by attracting migrants. In contrast, it benefits regions in Latin America, and especially Oceania, that are relatively sparsely populated and, in the baseline scenario, suffer large population losses and the correspondingly lower investments in technology due to global warming. Higher migration frictions make these places keep more of their population, and associated technology growth, as temperatures rise over time. Perhaps surprisingly, Central Africa, India, and China, all have larger losses from global warming when migration costs are large. The reason is that their high density and low income imply that much of the resulting increases in population concentrate there, leading to higher productivity growth but also lower amenities due to congestion.<sup>40</sup> The latter effect dominates in dense developing countries, but the former dominates in sparsely populated regions, like Oceania.

The right panel of Figure 15 presents the evolution of average welfare losses over time. The dashed lines present the overall effects for two different magnitudes of  $\vartheta$ . To help with the interpretation, we also present scenarios (solid lines) where we keep the evolution of temperature and population as in the baseline scenario. These exercises abstract from the feedback effect of temperatures and population on the economy. Comparing dashed and solid lines reveals the importance of these feedback effects. In the short-run, higher migration costs reduce economic activity leading to smaller temperature increases and smaller losses. In the long-run, in contrast, increases in population lead to more fossil fuel use, higher temperatures, and larger losses. Overall, larger migration costs lead to significantly larger losses from global warming. 25% larger migration costs lead to losses from temperature change that are more than a third larger by 2200. Over time, these differences decline, since in all scenarios carbon reserves are eventually depleted.

These results show that migration is indeed an essential adaptation mechanism. One that is quantitatively important, but differentially so across regions in the world. Ultimately, the best way to adapt to global warming is for agents to migrate to regions that lose less or even gain from temperature increases. Many of these regions are sparsely populated today, due to their lack of amenities and productivity, but could be improved as temperatures rise and new migrants invest in them over the next centuries.

---

<sup>40</sup>The implied increases in population that result from this large change in migration costs are as large as 6 billion people by 2150, stabilizing afterwards.

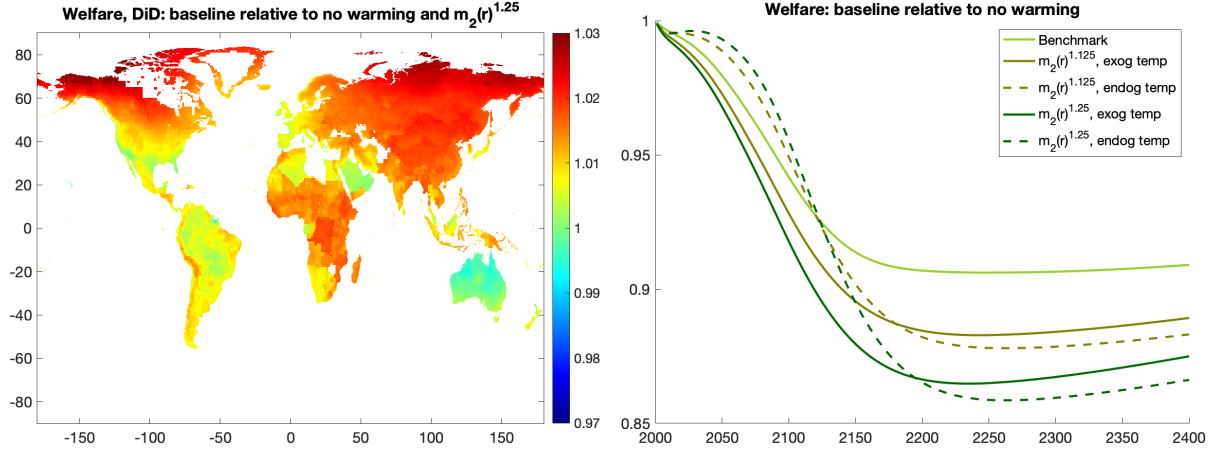


Figure 15: Welfare across different migration costs.

## 5.2 Trade

As with migration costs, we study the effect of global increases in commercial frictions that rise the bilateral iceberg trade costs  $\varsigma(\cdot, \cdot)$  to some power  $\vartheta > 1$ . Figure 16 presents the spatial and dynamic effect on welfare for values of  $\vartheta$  of 1.5 and 2. The left panel presents the spatial distribution of the relative effect of global warming on welfare in the baseline scenario with respect to the same relative effect in the scenario with higher trade costs. In this diff-and-diff calculation, large values, represented in red, identify areas that are hurt by larger trade costs. To understand the figure, it is important to realize that gravity in trade implies that most trade flows are very local. Because increases in temperatures are spatially correlated, areas that trade significantly with each other tend to experience similar shocks. This explains the small impact of trade on welfare in Figure 16.<sup>41</sup>

The spatial pattern in Figure 16 is markedly different than the one for migration. As with migration, larger trade costs make warming more harmful in Africa, India, and China. However, it also makes warming more harmful in Central and South America, as well as Europe, and less harmful in northern regions in Canada, Scandinavia, and Russia. Trade has little impact on northern regions since their relative isolation implies that they trade little with the rest of the world anyway. In contrast, regions in more central, well connected geographies, rely more on trade and so they suffer from the double impact of higher trade costs and higher temperatures. In addition, as with migration, higher trade costs reduce incomes which results in higher natality rates, particularly in the developed world, leading to additional congestion. Brazil, Africa, and India are affected the most.

The right panel of Figure 16 shows the temporal evolution of average welfare. As with migration, we plot cases keeping the evolution of temperatures and population constant, as well as the full equilibrium

<sup>41</sup>Importantly, our work abstracts from trade across industries due to local comparative advantage. If temperature affects the comparative advantage of regions, trade can play a much more important role as an adaptation mechanism. See Desmet and Rossi-Hansberg (2015), Nath (2020) and Conte et al. (2020) for studies that develop this mechanism.

evolution. The small effect of trade is evident, particularly when conditioning on the temperature path. Once we take the effect of changes in income and population on the evolution of temperature into account, we get smaller losses from global warming with higher trade costs in the short-run, but larger ones in the long-run. Similar to the case of changes in migration costs, lower incomes lead to smaller increases in temperature in the short-run, but larger population leads to greater losses from temperature rises in the long-run.<sup>42</sup> Overall, adaptation through trade seems to play only a minor role in our results.

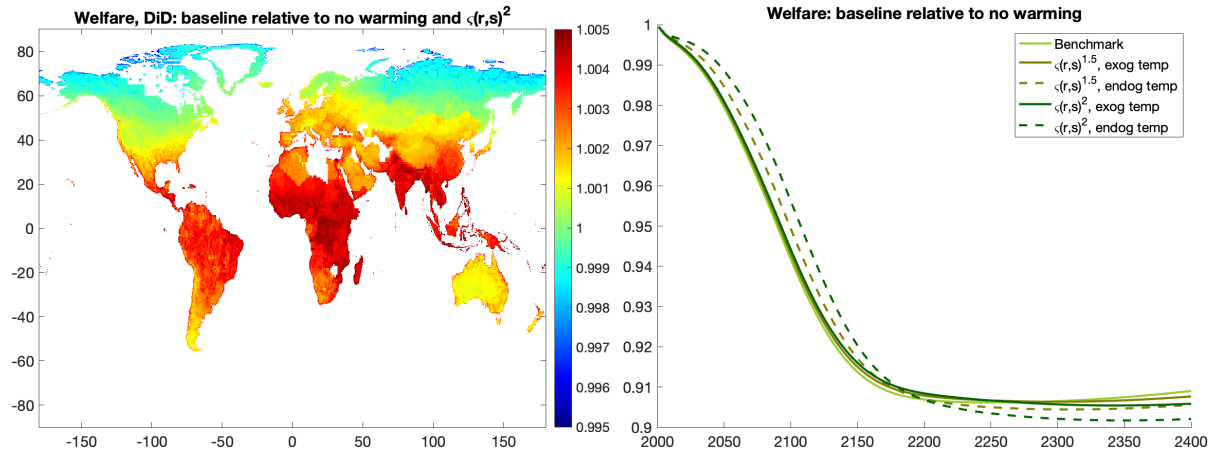


Figure 16: Welfare across different iceberg trade costs.

### 5.3 Innovation

The final adaptation mechanism we study in this section is innovation. Firm investments respond to market size and allow a region's technology to grow relative to that of other regions. Innovation improves northern regions' productivity, as they become warmer and gain population. It also accelerates the relative losses of regions that get too warm and lose market size due to the implied lower productivity and lower amenities. We study here the effect of lowering  $\gamma_1$  (or, equivalently, increasing  $\xi$ ). Changes in these parameters amount to changing the returns or cost of innovation proportionally across locations. Larger costs of innovation reduce real GDP growth and, therefore, growth in CO<sub>2</sub> emissions, curbing the temperature path. As with trade and migration costs, the lower real GDP growth pushes upwards natality rates and global population.

Figure 17 presents the spatial and dynamic implications of lower innovation returns (or higher innovation costs). The left panel presents the diff-and-diff for the welfare consequences of global warming in the baseline relative to the exercise with high innovation costs. The spatial pattern of this measure is simpler than the one for the other mechanisms. The upmost northern regions are hurt more (benefited less) by global warming when innovation costs are higher. Developing these areas by improving their productivity and moving economic activity to the north becomes more costly. The same phenomenon is apparent in the

<sup>42</sup>World population increases as much as 7 billion by 2200 when  $\vartheta = 2$ .

upmost southern regions, including Oceania and the southern tip of South America and Africa.

The right panel of Figure 17 presents the dynamic evolution of the cost of global warming. In all cases, with and without feedback effects from temperature, larger innovation costs lead to smaller losses from global warming. The reason is that larger innovation costs imply smaller benefits from density in locations that are eventually negatively affected by higher temperatures. In particular, Africa, India, and China experience lower technology growth and, therefore, attract less migrants from other locations. Given that these are the regions more affected by temperature rises, the average cost from this phenomenon declines. This effect builds up over time and is significant only after 2150. Once we incorporate the feedback effect through changes in the temperature and population paths, the lower temperature growth generates lower costs from global warming when innovation costs are larger even in the short-run.

These results illustrate the importance of studying the impact of adaptation mechanisms in a spatial model. The reason that higher innovation costs result in smaller costs from global warming is fundamentally spatial, as explained above. Overall, adaptation through innovation is an important mechanism, particularly in determining the spatial distribution of the welfare cost of global warming.

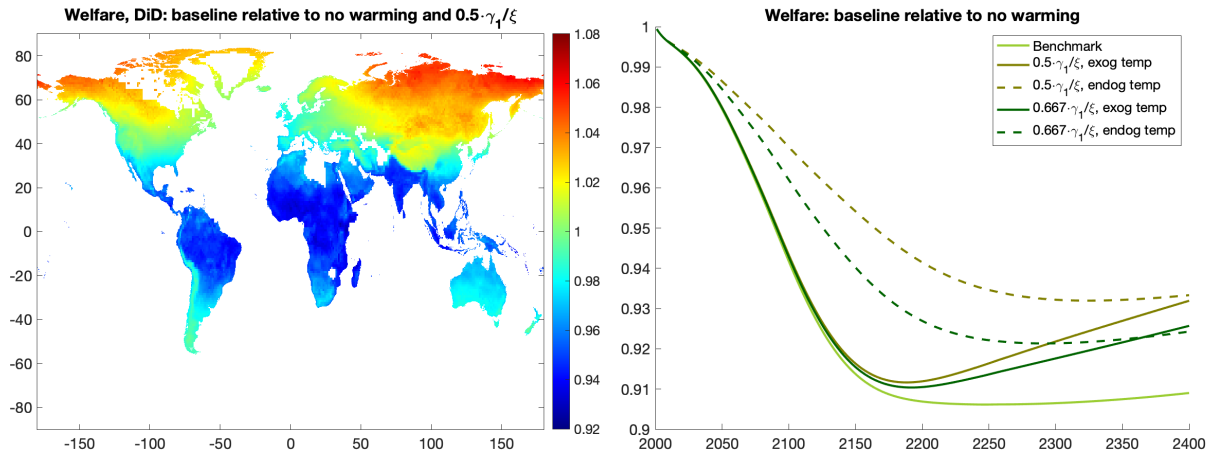


Figure 17: Welfare across different innovation costs.

## 6 Environmental Policies

Global warming constitutes a worldwide externality and so policy can potentially alleviate some of its negative economic impacts. Furthermore, in the model we have proposed, there are local and global technological externalities, as well as congestion costs, all of which imply that the competitive equilibrium is not efficient. Hence, in this framework, achieving the first best would require a number of policies that address these other sources of inefficiencies as well. This is in general hard, since such policies would require local and global dynamic policies that are currently unknown and, therefore, neither proposed nor implemented. In fact, in our framework, the mechanisms that make the firm's innovation decision effectively static in the

competitive equilibrium, do not imply the same for the planner's problem. Hence, solving for the optimal policy in our model, even without considering global warming is, so far, beyond our capabilities. Therefore, we proceed by evaluating some popular climate policies, rather than by designing optimal environmental policy.

A commonly proposed solution to the global carbon emission externality is to impose a global carbon tax,  $\tau$ , to increase the cost of fossil fuels and discourage their use. This follows the standard Pigouvian logic of using taxes or subsidies to equate the social and private marginal cost of fossil fuels.<sup>43</sup> In the same spirit, we also consider a common and global clean energy subsidy,  $s$ , that reduces the marginal cost of renewable energy. Thus, the cost of energy per unit of land becomes  $w_t(r)(1 + \tau)Q_t^f(r)e_t^{f,\omega}(r) + w_t(r)(1 - s)Q_t^c(r)e_t^{c,\omega}(r)$ .<sup>44</sup> We assume that the balance of taxes and subsidies is taxed or rebated lump sum at each location. Because carbon taxes delay the depletion of the stock of fossil fuels on Earth, we also study the potential gains from carbon taxes when an abatement technology is forthcoming. Finally, although mostly relegated to the appendix, we study the effect of policies that increase the elasticity of substitution between fossil and clean energy; for example, by encouraging the use of electric rather than gasoline vehicles.

## 6.1 Carbon Taxes

Figure 18 displays the evolution of CO<sub>2</sub> emissions and global temperatures when considering carbon taxes of 50%, 100% and 200%, keeping clean energy subsidies at zero.<sup>45</sup> As expected, carbon taxes reduce current consumption of fossil fuels at impact. For instance, a tax of 200% diminishes carbon emissions by 60% with respect to the benchmark scenario in the initial period. However, as the economy grows and the productivity of energy production increases, CO<sub>2</sub> emissions rise. Eventually, though, extraction costs increase sharply, and the price of fossil fuels relative to clean energy rises, generating a decline in CO<sub>2</sub> emissions. Carbon taxes not only reduce initial emissions but they also delay the year and the magnitude of the peak in CO<sub>2</sub> emissions. For example, with a tax of 200% the peak is 3.43 GtCO<sub>2</sub> lower and occurs 35 years later than in the scenario with no carbon taxes.

In sum, the main effect of a carbon tax is to delay dirty energy consumption, by spreading its use over time; less current consumption but more future consumption. The more protracted path for CO<sub>2</sub> emissions has stark implications for the evolution of global temperatures: It *flattens* the temperature curve. A carbon tax of 200% leads to an evolution of average global temperatures that is as much as 4°C lower in the first half of the 22nd century, peaks 100 years later at a temperature roughly 2°C lower, but eventually converges to the same temperature once the stock of carbon is depleted in both scenarios. This intertemporal CO<sub>2</sub>

<sup>43</sup>See Hassler et al. (2019) for a modern treatment and quantification of Pigouvian logic applied to climate policy.

<sup>44</sup>As already imposed in the notation and although potentially superior, we leave for future research an analysis of spatially heterogeneous policies or policies that vary over time. Such analysis is certainly feasible in our framework.

<sup>45</sup>Given that the price of fossil fuels in the initial period is on average 73 usd/tCO<sub>2</sub>, a carbon tax of 50% equals 37 usd/tCO<sub>2</sub>, similar to the maximum in the E.U. Emissions Trading Scheme; a carbon tax of 200% equals 146 usd/tCO<sub>2</sub>, close to the Swedish tax.



utilization pattern, governed in part by the convex cost of carbon extraction relative to clean energy, is essential in determining the effectiveness of carbon taxes. Carbon taxes tend to delay, not eliminate, the use of fossil fuels (even when the elasticity of substitution between fossil fuels and clean energy is rather large,  $\epsilon = 1.6$ , as in our calibration).

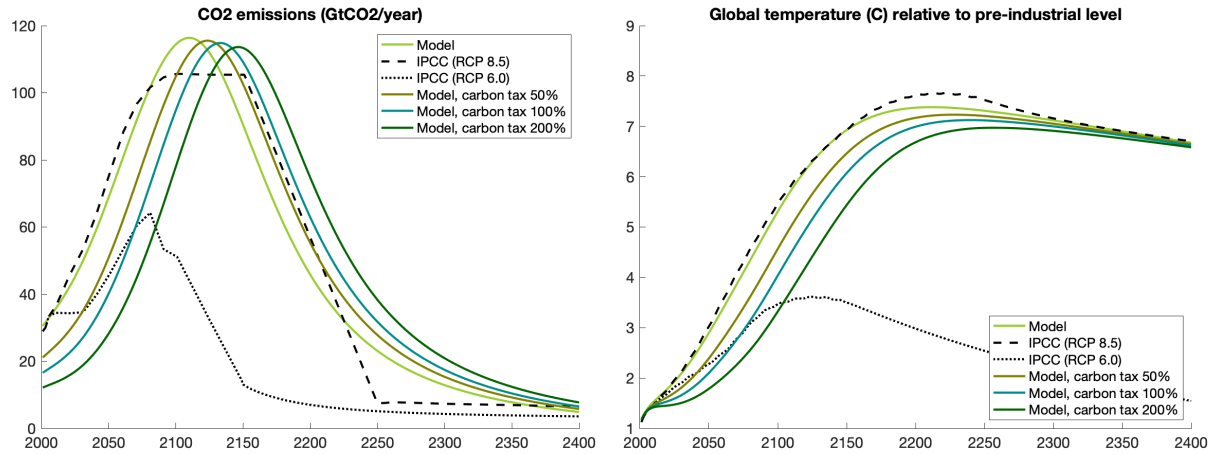


Figure 18: CO<sub>2</sub> emissions and global temperature under different carbon taxes.

Figure 19 presents global real GDP and welfare for each tax level relative to the baseline scenario with no environmental policy. At impact, the implementation of a uniform proportional carbon tax reduces the use of fossil fuels, which makes energy more expensive overall, and thus reduces income and welfare. The decline in welfare is less pronounced than that of real GDP, as welfare depends on real income which incorporates the lump sum transfer. Furthermore, initially, carbon taxes reduce firm innovation since potential current profits decline, and therefore reduce the growth rate of the economy. Of course, as time evolves, the flattening of the temperature curve has beneficial effects on amenities and productivities, leading to higher real income and welfare, as well as higher growth rates. Eventually, the curves in Figure 19 cross one, meaning that the implementation of the carbon tax is, on average, beneficial after that period. In the long-run, real GDP and welfare keep increasing due to a larger global population.<sup>46</sup>

The implementation of carbon taxes generates an intertemporal trade-off with short-term costs and long-term benefits. This naturally implies that any overall assessment of carbon policies depends on the chosen discount factor. Table 2 presents the global average real GDP and welfare losses from global warming across different tax levels and discount factors, with respect to a scenario in which environmental policies are absent. Our choice of discount factor is limited by the balanced-growth-path growth rate. In order to obtain finite present discounted values of welfare and real GDP for all future paths, we chose a baseline discount factor of  $\beta = 0.965$ .<sup>47</sup> For this value, carbon taxes are not desirable today. The largest present

<sup>46</sup>In the short-run, the implementation of carbon taxes reduces global income, rising natality rates. Consequently, global population is higher when we impose CO<sub>2</sub> levies.

<sup>47</sup>We also consider a value of  $\beta = 0.969$  that, given the balanced-growth-path growth rate of 0.03, implies that we value the relative



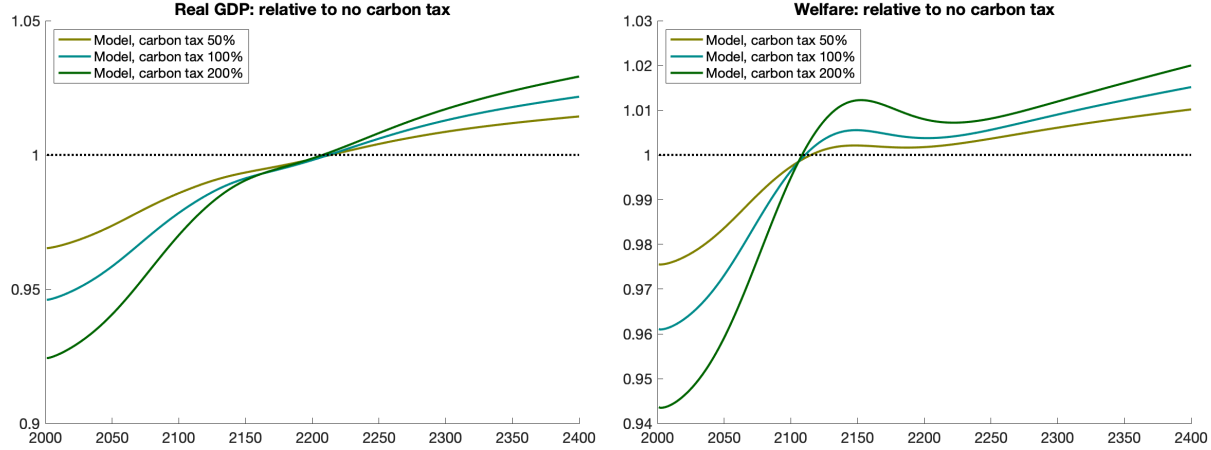


Figure 19: Real GDP and welfare under different carbon taxes.

discounted value of real GDP or welfare in Table 2 is obtained for  $\tau = 0$ . However, if we increase the discount factor to  $\beta = 0.969$ , a carbon tax of 200% or more maximizes welfare and real GDP. This large sensitivity of the optimal carbon tax is natural given the path shown in Figure 19 and cautions us not to rely too heavily on PDV statistics that depend on specific values of the discount factor. Ultimately, the discount factor used determines the policy-maker's preferences for the welfare of current versus future generations.

	PDV of real GDP			Welfare		
	BGP gr	$\beta=0.965$	$\beta=0.969$	BGP gr	$\beta=0.965$	$\beta=0.969$
$\tau=0\%$	3.043%	1	1	3.024%	1	1
$\tau=50\%$	3.048%	0.991	1.019	3.028%	0.997	1.016
$\tau=100\%$	3.050%	0.987	1.030	3.030%	0.995	1.024
$\tau=200\%$	3.053%	0.981	1.042	3.032%	0.993	1.033

Table 2: PDV of real GDP and welfare gains under different carbon taxes and discount factors.

The impact of carbon taxes is not only heterogeneous over time, but also across space. Figure 20 compares the welfare impact across locations of a carbon tax of 200%. As expected, the regions that are projected to gain from imposing the carbon tax are the regions that were projected to lose the most from global warming in Figure 8. Welfare gains from the tax range from 2% in South America, Central Africa, and South Asia; to losses of 6% in the coldest places, those expected to gain from higher temperatures. Two interesting exceptions are the Middle East and Algeria. They obtain relatively low gains from the global carbon tax, compared to their projected losses from global warming. The economy of those regions relies heavily on fossil fuel, so a carbon tax generates large distortions in production.<sup>48</sup>

gains in all period similarly.

<sup>48</sup>Appendix G.2 evaluates the role of carbon taxes in the worst-case-scenario for climate damages and Appendix I.1 develops further the discussion on the temporal and spatial effects of carbon taxes.

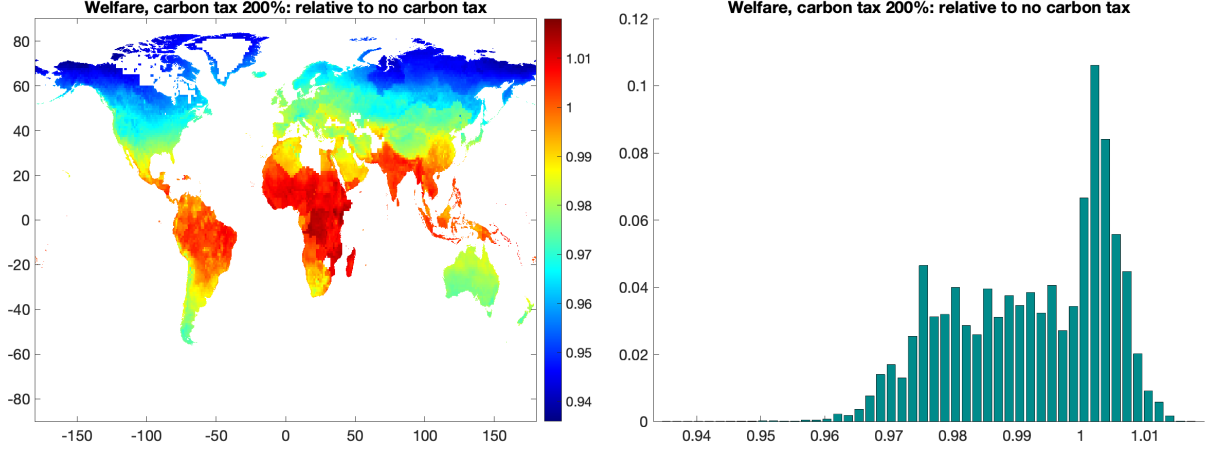


Figure 20: Local welfare effects of a carbon tax of 200% with a discount factor of  $\beta = 0.965$ .

## 6.2 Abatement

We have shown that the main effect of carbon taxes is to delay the use of fossil fuels, without affecting the total stock of carbon released to the atmosphere, thereby *flattening* the evolution of global temperatures over time. Of course, delaying CO<sub>2</sub> emissions, and flattening the temperature curve can be extremely beneficial if, at some point, humans invent an abatement technology that allows us to use fossil fuels without emitting CO<sub>2</sub> into the atmosphere (or capture CO<sub>2</sub> in the atmosphere through geoengineering). An abatement technology would eliminate, or reduce, the negative externality that results from the use of fossil fuels.<sup>49</sup> Since an abatement technology *cures* the economy from emitting CO<sub>2</sub> emissions after its invention, delaying the use of fossil fuels and flattening the temperature curve can become a very effective strategy, one that does affect total CO<sub>2</sub> emissions.<sup>50</sup> This is why carbon taxes and abatement technologies are complementary policies.

To illustrate this argument, here we consider a simple case in which an abatement technology becomes available at no cost in the year 2100.<sup>51</sup> Figure 21 introduces the abatement technology to the exercises repre-

<sup>49</sup>More precisely, if we denote by  $\nu_t(r)$  the share of CO<sub>2</sub> emissions abated in region  $r$  at period  $t$ , the evolution of atmospheric CO<sub>2</sub>, given by equation (18), becomes

$$S_{t+1} = S_{\text{pre-ind}} + \sum_{\ell=1}^{\infty} (1 - \delta_{\ell}) \left( E_{t+1-\ell}^{\prime f} + E_{t+1-\ell}^x \right) \quad (30)$$

$$E_t^{\prime f} = \int_S \int_0^1 (1 - \nu_t(r)) e_t^{f,\omega}(v) H(v) d\omega dv \quad (31)$$

The law of motion of fossil fuel extraction is still given by equation (10).

<sup>50</sup>The interaction of carbon taxes and an abatement technology within our framework is analogous to lock-downs and the introduction of a vaccine in a pandemia: a lockdown delays current infections at an economic cost, but reduces total infections only if a vaccine is forthcoming.

<sup>51</sup>As in Nordhaus (2015), we could alternatively assume that preventing a share  $\nu_t(r)$  of CO<sub>2</sub> emissions in region  $r$  at period  $t$  costs a fraction,  $(1 - \varpi_{1,t}(r) \cdot \nu_t(r)^{\varpi_2})$ , of household's income. We could assume that  $\varpi_{1,t}(r)$  declines over time to reflect the widening menu of technological alternatives and that it varies across regions depending on their carbon intensity. The parameter  $\varpi_2$  controls

sented in Figure 18. The solid curves present CO<sub>2</sub> emissions and global temperature under different carbon taxes when the abatement technology is not available. The dashed curves, present the results with the introduction of a perfect abatement technology in 2100. When the abatement technology is introduced, the flow of CO<sub>2</sub> into the atmosphere drops discontinuously and permanently to zero. The cut in the cumulative carbon dioxide emissions has transcendental consequences in the temperature path, which declines until it reaches a new and much lower steady-state.

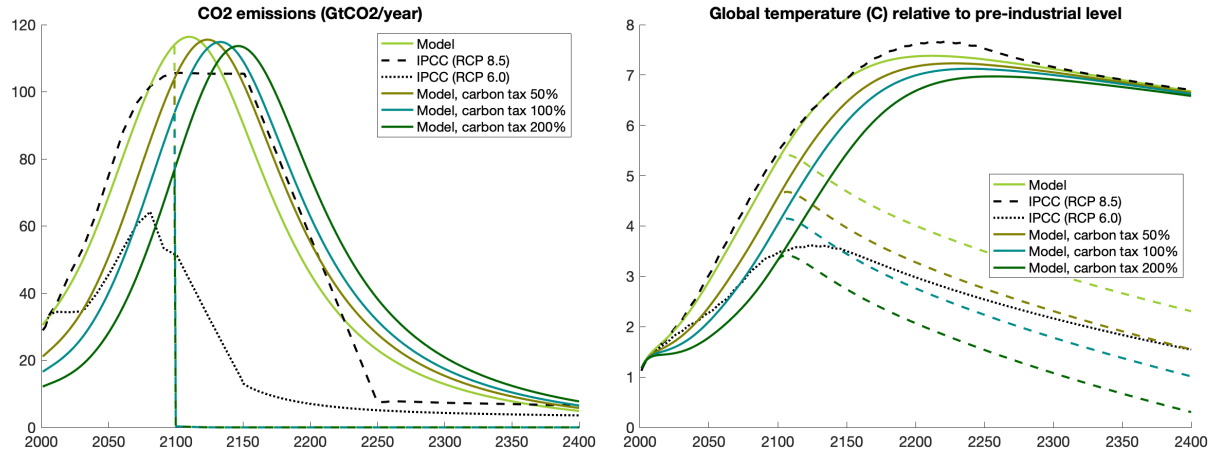


Figure 21: CO<sub>2</sub> emissions and global temperature under different carbon taxes, when considering the introduction of an abatement technology in 2100.

Figure 22 replicates Figure 19 but includes, in dashed lines, the global average real GDP and welfare effects of the implementation of a carbon tax relative to a scenario with no carbon taxes, when we introduce the abatement technology in 2100. Since the abatement technology eliminates the effect of carbon emission on temperatures, and therefore on amenities and productivity, the deceleration of growth caused by global warming that we observe after 2100 without an abatement technology is now avoided.<sup>52</sup>

Table 3 shows global average PDV of real GDP and welfare gains under the implementation of carbon taxes when an abatement technology becomes available in 2100. When comparing it with Table 2, we observe that, when an abatement technology is forthcoming, large carbon taxes are beneficial for the economy for both discount factors. With  $\beta = 0.969$ , the impact of this policy is very large and can yield gains in real GDP of more than 7% and in welfare of more than 8%. These results illustrate how the abatement technology and carbon taxes are complementary policies. That is, a forthcoming abatement technology makes

the degree of non-linearity in costs. At a global scale, Nordhaus (2015) considers  $\varpi_{1,t} = 0.0334$  and  $\varpi_2 = 2$ . Of course, because of well-understood free-rider problems, the abatement policy would still need to be imposed by a global agreement.

<sup>52</sup>Note that relative real GDP and welfare can be slightly lower in the abatement case for a couple of decades after the invention of the abatement technology. The reason is that the difference in temperatures between the benchmark scenario with and without abatement can be larger than the difference in temperature with and without abatement in the scenario with a carbon tax, depending on the second derivative of the temperature function at the time the abatement technology arrives. After a few decades, this effect is always dominated by the faster increases in temperature in the case without abatement.

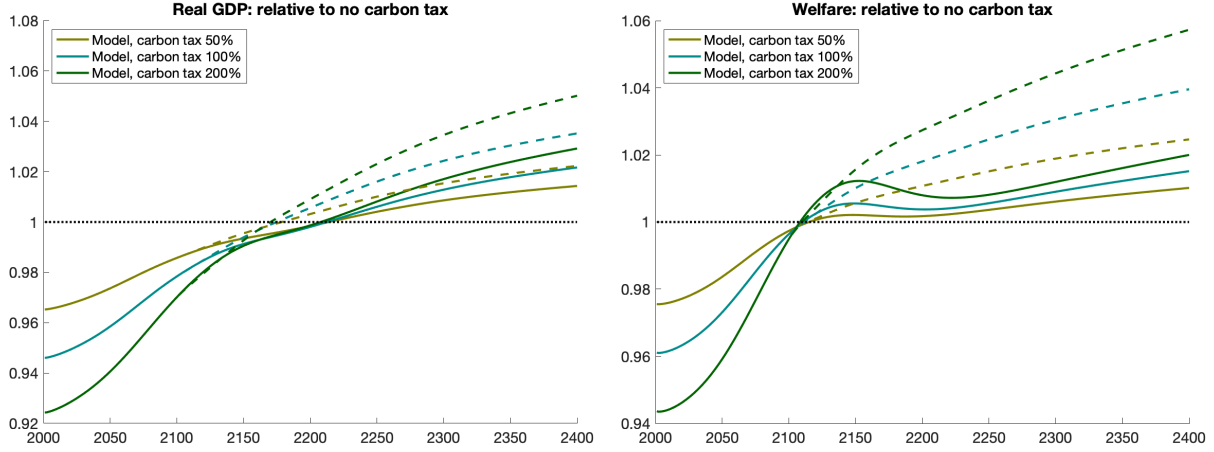


Figure 22: Real GDP and welfare under different carbon taxes, when considering the introduction of an abatement technology in 2100.

carbon taxes a much more effective policy. In fact, this combination of policies is the most effective one we have found in our analysis.<sup>53</sup>

	PDV of real GDP			Welfare		
	BGP gr	$\beta=0.965$	$\beta=0.969$	BGP gr	$\beta=0.965$	$\beta=0.969$
$\tau=0\%$	3.052%	1	1	3.037%	1	1
$\tau=50\%$	3.058%	0.994	1.031	3.043%	1.003	1.034
$\tau=100\%$	3.061%	0.992	1.050	3.046%	1.004	1.056
$\tau=200\%$	3.065%	0.989	1.074	3.051%	1.006	1.082

Table 3: PDV of real GDP and welfare gains under different carbon taxes and discount factors, when considering the introduction of an abatement technology in 2100.

### 6.3 Clean Energy Subsidies

Clean energy subsidies have two countervailing effects. First, they make clean energy less expensive, thereby creating incentives for agents to produce energy with clean sources. The magnitude of this effect is governed by the elasticity of substitution in energy production which we set at  $\epsilon = 1.6$ , as well as by the initial relative productivity of clean energy, which is heterogeneous across locations and chosen to match relative energy use. Second, clean energy subsidies reduce the price of the energy composite. This additional effect is also governed by the share of clean energy in the energy composite, which is initially about 12%. Figure 23 shows that in the quantitative model we have put forward, these two effects roughly

<sup>53</sup>Appendix I.3 provides additional results and Appendix I.4 quantifies the welfare benefits when the abatement technology becomes available one century later.

cancel out. Subsidies as large as 75% yield only a minuscule reduction in CO<sub>2</sub> emission and temperatures. We conclude that clean energy subsidies are not an effective way to combat global warming.<sup>54</sup>

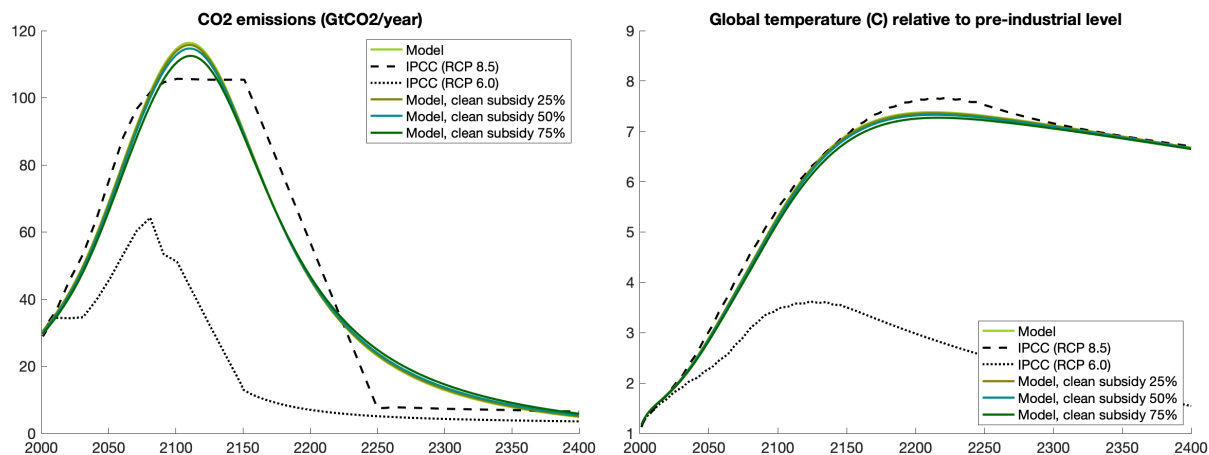


Figure 23: CO<sub>2</sub> emissions and global temperature under different clean energy subsidies.

At impact, the subsidy on clean energy leads to a reduction in the composite price of energy. Given our Cobb-Douglas production function, the subsidy acts like a positive production subsidy that increases output and encourages innovation, which accelerates growth. Given that the model features dynamic spillovers that are not internalized in equilibrium, such a subsidy is potentially beneficial. Furthermore, the subsidy leads to declines in energy costs that varies across locations. Areas using more clean energy relatively to fossil fuels undergo greater declines in the composite price of energy. On average, developed countries tend to be more intensive in clean energy, attracting more households to those places. The re-location of people towards the most productive places rises global real GDP and welfare, but also lowers natality rates and world population in the long-run. A lower population in the balanced growth path leads to lower long-run growth rates. In sum, subsidies increase output and welfare in the short-run, but eventually reduce them in the long-run. As with carbon taxes, the overall economic effects from the subsidy depend on the discount factor. In this case, however, the sign of the short- and long-run effects are reversed relative to the carbon tax. Larger discount factors result in smaller gains or losses. Table 4 presents these results.

Figure 24 presents the spatial distribution of welfare gains from a 75% clean energy subsidy relative to the baseline. The left panel shows the heterogeneous spatial effects from the subsidy. As we discussed above, the subsidy has only a small impact on the temperature path. The main source of spatial heterogeneity comes from the differences in the relative price of fossil fuels and clean energy. Remember that, in the quantification of our model, we infer this relative price using the relative use of energy sources, which is available at the country level only (which explains the national demarcations in the figure). Scandinavia has a large relative price of fossil fuels (partly because of other prevailing policies) and so it benefits more

<sup>54</sup>Appendix I.2 evaluates the joint effect of carbon taxes and clean energy subsidies.

	PDV of real GDP			Welfare		
	BGP gr	$\beta=0.965$	$\beta=0.969$	BGP gr	$\beta=0.965$	$\beta=0.969$
$s=0\%$	3.043%	1	1	3.024%	1	1
$s=25\%$	3.040%	1.011	1.009	3.020%	1.007	1.000
$s=50\%$	3.034%	1.032	1.021	3.012%	1.020	0.996
$s=75\%$	3.012%	1.094	1.044	2.989%	1.050	0.975

Table 4: PDV of real GDP and welfare gains under different clean energy subsidies and discount factors.

from the subsidy than the Arabian peninsula or Australia, where fossil fuels are relatively cheap. Paraguay benefits significantly, since clean energy is cheap there due to the abundance of hydroelectric power. The right panel presents the distribution of welfare gains. Parts of Africa and South America gain in welfare more than 6%, while some regions in North Africa or the Arabian peninsula gain only 2%. Higher discount factors would make some of these regions lose.

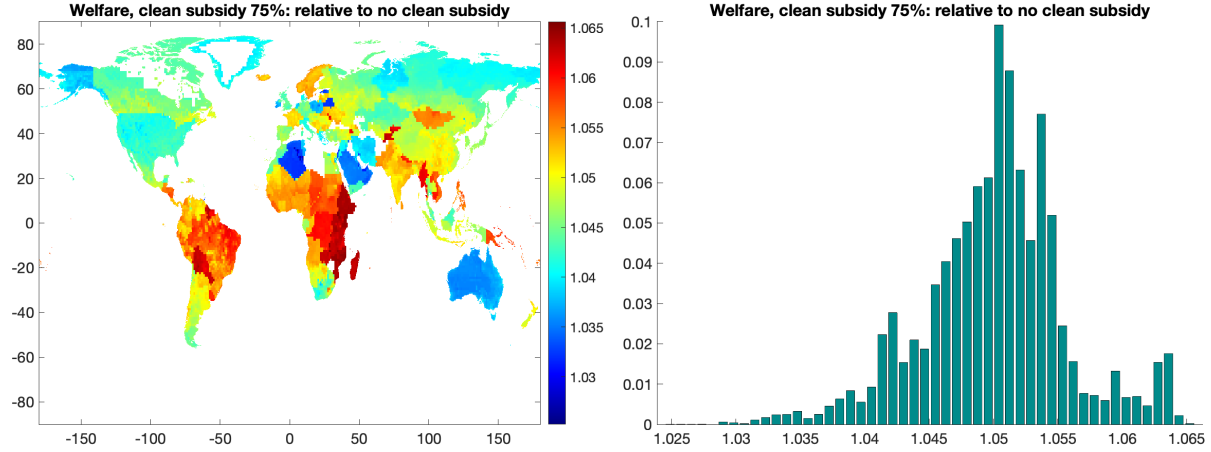


Figure 24: Local welfare effects of a clean energy subsidy of 75% with a discount factor of  $\beta = 0.965$ .

## 7 Conclusions

The goal of this paper is to propose a novel geographically detailed integrated assessment model of the effect of global warming on economic outcomes and welfare. The large heterogeneity in projected temperature changes across regions of the world, and the heterogeneous effects of these changes across locations and over time, underscore the need for assessment models that feature a realistic geography with many locations and agents that make decisions to live, move, trade, and invest across them. The micro-founded spatial dynamic model that forms the core of the proposed framework features local population growth, costly migration and trade, endogenous technology investments, as well as local fossil and energy use and its impact on local temperature and, correspondingly, its heterogeneous effect on amenities and productiv-

ity. Thus, the proposed model allows us to incorporate a number of endogenous adaptation mechanisms that have been mostly absent in assessment models so far. Furthermore, it allows us to estimate the impact of global warming on economic outcomes by explicitly aggregating the dynamic effects on local outcomes.

When we quantify the proposed economic model for the world economy at a fine level of spatial resolution we obtain local effects of global warming on welfare that range from losses of 15% to gains of 14%. We find that the distribution of relative losses across locations is fairly robust to the damage functions we estimate but, in contrast, our estimates imply large uncertainty about overall welfare losses. The 95% confidence interval of average welfare losses in 2200 ranges from losses of 20% to zero. This wide range reflects the reality that, although the data allows us to estimate significant effects from temperature on fundamental productivity and amenities, the estimates are still imprecise given that the rise in temperatures has only recently started to affect economic outcomes more severely.

The model we propose can be used as a workhorse model to study a number of additional dimensions of climate change as well as alternative policies. A few examples are coastal flooding, as analyzed in [Desmet et al. \(2021\)](#), the increased likelihood of extreme weather events, or the political economy of climate policy as determined by the spatially heterogeneous effects we have uncovered.

Inevitably, our model abstracts from some important aspects. First, the model we propose does not introduce multiple sectors and the effect of temperature on relative sectoral productivity. [Conte et al. \(2020\)](#) show how this can be done in a related framework. Second, we have abstracted from purposeful innovations in green, fossil, and abatement technologies. In our model these technologies only evolve through spillovers from other innovations. Third, the model we develop gains tractability from assuming an economic structure in which anticipatory effects from future shocks or policy only affect land rents, but do not affect allocations. That is, future events do not affect the spatial evolution of the economy. Incorporating anticipatory effects in rich spatial model with endogenous investments and growth is still infeasible, although potentially interesting. Of course, the importance of anticipatory effects to evaluate protracted phenomena, like global warming, is debatable.

Global warming presents a daunting challenge for humanity. Designing the best tools to address it requires modern micro-founded economic models that incorporate multiple forms of adaptation and the rich spatial heterogeneity of the world. Our hope is that this paper contributes to this effort.

## References

- Acemoglu, D., Aghion, P., Barrage, L., and Hemous, D. (2019). Climate change, directed innovation, and energy transition: The long-run consequences of the shale gas revolution.
- Acemoglu, D., Aghion, P., Bursztyn, L., and Hemous, D. (2012). The environment and directed technical change. *American Economic Review*, 102(1):131–66.
- Acemoglu, D., Akcigit, U., Hanley, D., and Kerr, W. (2016). Transition to clean technology. *Journal of Political Economy*, 124(1):52–104.
- Albouy, D., Graf, W., Kellogg, R., and Wolff, H. (2016). Climate amenities, climate change, and american quality of life. *Journal of the Association of Environmental and Resource Economists*, 3(1):205–246.
- Allen, T. and Arkolakis, C. (2014). Trade and the topography of the spatial economy. *The Quarterly Journal of Economics*, 129(3):1085–1140.
- Anthoff, D. and Tol, R. (2014). The climate framework for uncertainty, negotiation and distribution (fund), technical description, version 3.9.
- Auffhammer, M. (2018). Quantifying economic damages from climate change. *Journal of Economic Perspectives*, 32(4):33–52.
- Balboni, C. (2019). *In harm's way? Infrastructure investments and the persistence of coastal cities*. PhD thesis.
- Barrage, L. (2019). Optimal Dynamic Carbon Taxes in a Climate–Economy Model with Distortionary Fiscal Policy. *The Review of Economic Studies*, 87(1):1–39.
- Barreca, A., Clay, K., Deschenes, O., Greenstone, M., and Shapiro, J. S. (2016). Adapting to climate change: The remarkable decline in the us temperature-mortality relationship over the twentieth century. *Journal of Political Economy*, 124(1):105–159.
- Bauer, N., Hilaire, J., Brecha, R. J., Edmonds, J., Jiang, K., Kriegler, E., Rogner, H.-H., and Sferra, F. (2017). Data on fossil fuel availability for shared socioeconomic pathways. *Data in Brief*, 10:44 – 46.
- Baylis, P. (2020). Temperature and temperament: Evidence from twitter. *Journal of Public Economics*, 184:104161.
- Becker, G. (1960). An economic analysis of fertility. In *Demographic and Economic Change in Developed Countries*, pages 209–240. National Bureau of Economic Research, Inc.
- Benveniste, H., Oppenheimer, M., and Fleurbaey, M. (2020). Effect of border policy on exposure and vulnerability to climate change. *Proceedings of the National Academy of Sciences*.



- Bernard, A. B., Eaton, J., Jensen, J. B., and Kortum, S. (2003). Plants and productivity in international trade. *American Economic Review*, 93(4):1268–1290.
- Bosetti, V., Massetti, E., and Tavoni, M. (2007). The WITCH Model. Structure, Baseline, Solutions. Technical report.
- Boucher, O. and Reddy, M. (2008). Climate trade-off between black carbon and carbon dioxide emissions. *Energy Policy*, 36(1):193–200.
- BP (2019). Bp statistical review of world energy.
- Burke, M., Hsiang, S. M., and Miguel, E. (2015a). Climate and conflict. *Annual Review of Economics*, 7(1):577–617.
- Burke, M., Hsiang, S. M., and Miguel, E. (2015b). Global non-linear effect of temperature on economic production. *Nature*, 527:235–239.
- Carleton, T. A., Jina, A., Delgado, M. T., Greenstone, M., Houser, T., Hsiang, S. M., Hultgren, A., Kopp, R. E., McCusker, K. E., Nath, I. B., Rising, J., Rode, A., Seo, H. K., Viaene, A., Yuan, J., and Zhang, A. T. (2020). Valuing the global mortality consequences of climate change accounting for adaptation costs and benefits. Working Paper 27599, National Bureau of Economic Research.
- Carlino, G. A., Chatterjee, S., and Hunt, R. M. (2007). Urban density and the rate of invention. *Journal of Urban Economics*, 61(3):389 – 419.
- Carrea, L., Embury, O., and Merchant, C. J. (2015). Datasets related to in-land water for limnology and remote sensing applications: distance-to-land, distance-to-water, water-body identifier and lake-centre co-ordinates. *Geoscience Data Journal*, 2(2):83–97.
- Colella, F., Lalive, R., Sakalli, S. O., and Thoenig, M. (2019). Inference with arbitrary clustering.
- Conley, T. (1999). Gmm estimation with cross sectional dependence. *Journal of Econometrics*, 92(1):1 – 45.
- Conte, B., Desmet, K., Krisztián, D., and Rossi-Hansberg, E. (2020). Local sectoral specialization in a warming world. Technical report.
- Correia, S. (2016). Linear models with high-dimensional fixed effects: An efficient and feasible estimator. Technical report. Working Paper.
- Costinot, A., Donaldson, D., and Smith, C. (2016). Evolving Comparative Advantage and the Impact of Climate Change in Agricultural Markets: Evidence from 1.7 Million Fields around the World. *Journal of Political Economy*, 124(1):205–248.
- Crippa, M., Guizzardi, D., Muntean, M., Olivier, J., Schaaf, E., Solazzo, E., and Vignati, E. (2019). Fossil co2 and ghg emissions of all world countries.

- Dell, M., Jones, B. F., and Olken, B. A. (2012). Temperature shocks and economic growth: Evidence from the last half century. *American Economic Journal: Macroeconomics*, 4(3):66–95.
- Dell, M., Jones, B. F., and Olken, B. A. (2014). What do we learn from the weather? the new climate–economy literature. *Journal of Economic Literature*, 52(3):740–798.
- Delventhal, M. J., Fernández-Villaverde, J., and Guner, N. (2019). Demographic transitions across time and space.
- Deschênes, O. and Greenstone, M. (2007). The economic impacts of climate change: Evidence from agricultural output and random fluctuations in weather. *American Economic Review*, 97(1):354–385.
- Desmet, K., Kopp, R. E., Kulp, S. A., Nagy, D. K., Oppenheimer, M., Rossi-Hansberg, E., and Strauss, B. H. (2021). Evaluating the economic cost of coastal flooding. *American Economic Journal: Macroeconomics*.
- Desmet, K., Nagy, D. K., and Rossi-Hansberg, E. (2018). The geography of development. *Journal of Political Economy*, 126(3):903–983.
- Desmet, K. and Rappaport, J. (2017). The settlement of the United States, 1800–2000: The long transition towards Gibrat’s law. *Journal of Urban Economics*, 98(C):50–68.
- Desmet, K. and Rossi-Hansberg, E. (2014). Spatial development. *American Economic Review*, 104(4):1211–43.
- Desmet, K. and Rossi-Hansberg, E. (2015). On the spatial economic impact of global warming. *Journal of Urban Economics*, 88(C):16–37.
- Dietz, S. and Lanz, B. (2020). Can a growing world be fed when the climate is changing? Technical report.
- Eaton, J. and Kortum, S. (2002). Technology, geography, and trade. *Econometrica*, 70(5):1741–1779.
- Etminan, M., Myhre, G., Highwood, E. J., and Shine, K. P. (2016). Radiative forcing of carbon dioxide, methane, and nitrous oxide: A significant revision of the methane radiative forcing. *Geophysical Research Letters*, 43(24):12,614–12,623.
- Forster, P., Ramaswamy, V., Artaxo, P., Berntsen, T., Betts, R., Fahey, D., Haywood, J., Lean, J., Lowe, D., Myhre, G., Nganga, J., Prinn, R., Raga, G., Schulz, M., Dorland, R., Bodeker, G., Boucher, O., Collins, W., Conway, T., and Whorf, T. (2007). *Changes in Atmospheric Constituents and in Radiative Forcing*.
- Fried, S. (2019). Seawalls and stilts: A quantitative macro study of climate adaptation. 2019 Meeting Papers 898, Society for Economic Dynamics.
- Gaedicke, C., Franke, D., Ladage, S., Lutz, R., Pein, M., Rebscher, D., Schauer, M., Schmidt, S., and von Goerne, G. (2020). Data and developments concerning german and global energy supplies. Technical report.

- Golosov, M., Hassler, J., Krusell, P., and Tsyvinski, A. (2014). Optimal taxes on fossil fuel in general equilibrium. *Econometrica*, 82(1):41–88.
- Graff-Zivin, J. and Neidell, M. (2014). Temperature and the allocation of time: Implications for climate change. *Journal of Labor Economics*, 32(1):1–26.
- Greenwood, J., Hercowitz, Z., and Krusell, P. (1997). Long-run implications of investment-specific technological change. *American Economic Review*, 87(3):342–62.
- Hassler, J., Krusell, P., and Olovsson, C. (2018). The consequences of uncertainty: Climate sensitivity and economic sensitivity to the climate. *Annual Review of Economics*, 10(1):189–205.
- Hassler, J., Krusell, P., and Olovsson, C. (2019). Directed technical change as a response to natural-resource scarcity. Working Paper Series 375, Sveriges Riksbank (Central Bank of Sweden).
- Hope, C. and Hope, M. (2013). The social cost of co<sub>2</sub> in a low-growth world. *Nature Climate Change*, 3:722–724.
- IEA (2019). *World Energy Outlook 2019*.
- IEA (2020). Co<sub>2</sub> emissions from fuel combustion. Technical report. Database Documentation.
- IPCC (2007). Climate change 2007: Synthesis report. contribution of working groups i, ii and iii to the fourth assessment report of the intergovernmental pan on climate change. *Cambridge University Press*.
- IPCC (2013). Climate change 2013: The physical science basis. contribution of working group i to the fifth assessment report of the intergovernmental panel on climate change. *Cambridge University Press*.
- Joos, F., Roth, R., Fuglestedt, J. S., Peters, G. P., Enting, I. G., von Bloh, W., Brovkin, V., Burke, E. J., Eby, M., Edwards, N. R., Friedrich, T., Frölicher, T. L., Halloran, P. R., Holden, P. B., Jones, C., Kleinen, T., Mackenzie, F. T., Matsumoto, K., Meinshausen, M., Plattner, G.-K., Reisinger, A., Segschneider, J., Shaffer, G., Steinacher, M., Strassmann, K., Tanaka, K., Timmermann, A., and Weaver, A. J. (2013). Carbon dioxide and climate impulse response functions for the computation of greenhouse gas metrics: a multi-model analysis. *Atmospheric Chemistry and Physics*, 13(5):2793–2825.
- Krusell, P. and Smith, A. (2017). Climate change around the world. 2017 Meeting Papers 1582, Society for Economic Dynamics.
- Kummu, M., Taka, M., and Guillaume, J. (2018). Gridded global datasets for gross domestic product and human development index over 1990–2015. *Scientific Data*, 5:180004.
- Lucas, R. E. (1976). Econometric policy evaluation: A critique. *Carnegie-Rochester Conference Series on Public Policy*, 1:19 – 46.

- Mcglade, C. and Ekins, P. (2015). The geographical distribution of fossil fuels unused when limiting global warming to 2c. *Nature*, 517:187–90.
- Missirian, A. and Schlenker, W. (2017). Asylum applications respond to temperature fluctuations. *Science*, 358(6370):1610–1614.
- Mitchell, T. (2003). Pattern scaling: An examination of the accuracy of the technique for describing future climates. *Climatic Change*, 60:217–242.
- Monte, F., Redding, S. J., and Rossi-Hansberg, E. (2018). Commuting, migration, and local employment elasticities. *American Economic Review*, 108(12):3855–90.
- Myhre, G., Highwood, E. J., Shine, K. P., and Stordal, F. (1998). New estimates of radiative forcing due to well mixed greenhouse gases. *Geophysical Research Letters*, 25(14):2715–2718.
- Nath, I. (2020). The food problem and the aggregate productivity consequences of climate change. *Job Market Paper*.
- Nordhaus, W. (2015). Climate clubs: Overcoming free-riding in international climate policy. *American Economic Review*, 105(4):1339–70.
- Nordhaus, W. and Boyer, J. (2002). Economic models of global warming. mit press, cambridge mass., 2000. isbn 0 262 14071 3. *Environment and Development Economics*, 7(3):593–601.
- Nordhaus, W. D. (2006). Geography and macroeconomics: New data and new findings. *Proceedings of the National Academy of Sciences*, 103(10):3510–3517.
- Nordhaus, W. D. (2017). Revisiting the social cost of carbon. *Proceedings of the National Academy of Sciences*, 114(7):1518–1523.
- Papageorgiou, C., Saam, M., and Schulte, P. (2017). Substitution between clean and dirty energy inputs: A macroeconomic perspective. *The Review of Economics and Statistics*, 99(2):281–290.
- Popp, D. (2004). Entice: endogenous technological change in the dice model of global warming. *Journal of Environmental Economics and Management*, 48(1):742 – 768.
- Popp, D. (2006). Entice-br: The effects of backstop technology rd on climate policy models. *Energy Economics*, 28(2):188 – 222.
- Redding, S. J. and Rossi-Hansberg, E. (2017). Quantitative spatial economics. *Annual Review of Economics*, 9(1):21–58.
- Rogner, H.-H. (1997). An assessment of world hydrocarbon resources. *Annual Review of Energy and the Environment*, 22(1):217–262.

- Schlenker, W. and Roberts, M. J. (2009). Nonlinear temperature effects indicate severe damages to u.s. crop yields under climate change. *Proceedings of the National Academy of Sciences*, 106(37):15594–15598.
- Schwerhoff, G. and Stuermer, M. (2020). Non-renewable resources, extraction technology, and endogenous growth. Working Papers 1506.
- Simonovska, I. and Waugh, M. (2014). The elasticity of trade: Estimates and evidence. *Journal of International Economics*, 92(1):34–50.
- Stern, D. I. (2012). Interfuel substitution: A meta-analysis. *Journal of Economic Surveys*, 26(2):307–331.
- UN (2004). The united nations on world population in 2300. *Population and Development Review*, 30(1):181–187.
- UN (2019). *World Population Prospects 2019: Data Booklet*.
- Zabreyko, P. P., Koshelev, A., Krasnoselskii, M., Mikhlin, S., Rakovshchik, L. S., Stet’senko, V., Shaposhnikova, T., and Anderssen, R. (1975). *Integral equations: A reference text*.